A Spacetime Approach to Defining Vacuum States and Entropy

by

Yasaman Kouchekzadeh Yazdi

A thesis
presented to the University of Waterloo
in fulfillment of the
thesis requirement for the degree of
Master of Science
in
Physics

Waterloo, Ontario, Canada, 2013

I hereby declare that I am the sole author of this thesis. This is a true copy of the thesis, including any required final revisions, as accepted by my examiners.

I understand that my thesis may be made electronically available to the public.

Abstract

We apply a recent proposal for a distinguished ground state of a quantum field in a globally hyperbolic spacetime to the free massless scalar field in a causal diamond in two-dimensional Minkowski space. We investigate the two limits in which the Wightman function is evaluated (i) for pairs of points that lie in the centre of the diamond (i.e. far from the boundaries), and (ii) for pairs of points that are close to the left or right corner. We find that in the centre, the Minkowski vacuum state is recovered, with a definite value of the infrared cutoff. Interestingly, the ground state is not the Rindler vacuum in the corner of the diamond, as might have been expected, but is instead the vacuum of a flat space in the presence of a static mirror on that corner. We confirm these results by numerically evaluating the Wightman function of a massless scalar field on a causal set corresponding to the continuum causal diamond. We also present an independent calculation of the entanglement entropy for a free massless scalar field in 1+1 dimensions. We use a recent formula for a global expression of entropy using Green functions of the theory. This formula is independent of a density matrix with respect to a hypersurface (as the usual definition of entropy depends on), and it is applicable to both continuum spacetimes and to discrete causal sets. We compute the entanglement entropy in a spacetime of two causal diamonds in the continuum and in a causal set, in the limit that one is much larger than the other. In the continuum, we obtain the result $S = \frac{1}{3}\ln\left(\frac{\ell}{a}\right) + c$, where a is the UV cutoff of the theory, ℓ is the diameter of the smaller diamond, and c is a constant. This result is in agreement with results in CFT.

Acknowledgements

I would like to thank Niayesh Afshordi and Rafael Sorkin for their supervision. Their insight, guidance, and support, taught me a lot and made research very enjoyable for me.

I would also like to thank my friends, colleagues, and collaborators, including Fay Dowker, David Rideout, Siavash Aslanbeigi, Mehdi Saravani, and Michel Buck, for many insightful discussions. In addition, I thank the other members of my committees, Latham Boyle, Robb Mann, and Rob Myers, for helpful feedback on my research.

I thank my family, and my friends, especially Farbod, Miguel, Sharad, and Laura.

Finally, I thank my love, Anton.

Dedication

This is dedicated to Babashi.

Table of Contents

List of Figures

Chapter 1

Introduction

Taking the relativistic view that the physical world has a space-time character requires an approach to quantum field theory that is built on spacetime concepts, one that makes no fundamental appeal to "time as a parameter." The approach of algebraic quantum field theory takes this view seriously and attempts to push the foundations towards greater covariance, basing the theory on appropriate algebras of operators associated to open spacetime regions. The focus on the quasi-local algebras as the central constructs of the theory has encouraged the point of view that in general in curved spacetime there is no preferred quantum state and that a choice of state is akin to a choice of coordinates (see *e.g.* [50]). However, the algebraic approach has not been completely successful in constructing the expectation value of the stress-energy tensor or dealing with interacting fields.

With that in mind, an open question is whether quantum field theory requires in addition the identification of a distinguished "ground state" (or class of them). A ground state for a quantum field is its lowest energy state. It plays a very important role in the description and determination of a quantum system's evolution. One cannot, for example, speak of particles without first having a ground state defined. However, the ground state is in general very difficult to define, especially in the presence of gravity.

This work addresses this question. There has been a recent proposal for defining a distinguished ground state in a general globally hyperbolic spacetime (this includes globally hyperbolic regions in a larger spacetime) [27, 30]. The Wightman or two-point function, $W(X, Y)$, of this "Sorkin-Johnston" (SJ) ground state is defined in an essentially covariant way starting from $\Delta(X, Y)$, the Pauli-Jordan function or commutator function. The SJ

proposal is in contrast to conventional ways of choosing a vacuum state, which usually rely on the existence of symmetries in the spacetime.

In the SJ proposal, the Pauli-Jordan function is treated as an integral operator over the Hilbert space of square integrable functions in the region of spacetime being considered. The Wightman function of the quantised field, and therefore the vacuum state of the theory, is defined by restricting to the positive eigenspace of this operator when it is self-adjoint. As mentioned, an important feature of this prescription is that it is covariant. This proposal originated from efforts by R. Sorkin and S. Johnston to develop scalar field theory on a causal set and was later realized to have an equally important application in continuum spacetimes as well.

In this work, we study the SJ proposal in particular for the case of a free massless scalar field in flat spacetime. We look at Minkowksi and Rindler spacetimes, and we take a detailed look at the proposal applied to the spacetime of a causal diamond of two-dimensional Minkowski spacetime. We pay particular attention to the Wightman function obtained in the limit where the size of the diamond is large compared to the geodesic separation between the two arguments of W, and where spacetime points lie either (i) far away from the left and right corners or (ii) close to one of the corners.

In the former limit one might hope to recover the unique Poincaré-invariant Minkowski vacuum state, if such a state existed. But in fact, no such vacuum exists, since W is logarithmic and depends on an arbitrary length-parameter or "infrared cutoff". In our finite diamond, we find that W has the expected form, but with a definite value of the length-parameter determined by the diamond's area.

In the latter limit, one might expect to see the Rindler vacuum state, since the geometry of the corner approaches that of the familiar Rindler wedge as the diamond size tends to infinity. However, we find that this is not the case. Instead, the SJ state close to the corner is the vacuum state of Minkowski spacetime with a static mirror on the corner.

Further, we use the original causal set QFT formulation [26] to construct the ground state on a causal set that approximates the continuum causal diamond. We compare the results with the foregoing continuum analysis in the subregions of the causal set corresponding to the two limits (i) and (ii). In both cases, the Wightman function on the causal set is in good agreement with the continuum Wightman function.

A second question that we address is whether a description of entropy can be formulated without reference to a state on a hypersurface (as the usual definition of entropy depends

on). This would be useful for example in cases where a quantum field does not admit a meaningful restriction to a hypersurface. As mentioned in the opening discussion, in the relativistic view it would be ideal to move towards a description of spacetime quantities in terms of spacetime concepts. It may also turn out to be necessary to disregard the notion of state on a hypersurface in quantum gravity, and in particular, in causal set theory which we consider here. There has recently been found a formula for the entropy of a spacetime region, for a free scalar field theory, that uses correlation functions of the field [43].

Again, we take a detailed look at this formula applied to the spacetime of causal diamonds in 1+1 Minkowski spacetime, for both the continuum theory and the causal set theory. We consider the entanglement entropy resulting from considering a smaller causal diamond subregion of the larger one, in a limit where the size of the larger diamond is much greater than the size of the smaller one. We expect to obtain the results of calculations done in CFT, where the entanglement between a shorter interval and a longer one is computed, the intervals being the Cauchy surfaces or diameters of our causal diamonds. Further understanding is required to interpret the results we obtain in the causal sets. In the continuum we obtain results in agreement with those in CFT.

We begin with a short chapter introducing causal set theory, followed by chapters discussing the proposal for the SJ ground state and the formula for entropy.

Chapter 2

Causal Set Theory

Quantum gravity aims to find a unified framework for quantum mechanics and general relativity, and it remains an important open problem in physics. Causal set theory is an approach to quantum gravity.

A causal set, or causet, is a set $\mathcal{C}$ together with an ordering relation $\preceq$ that satisfies the following conditions:

- It is reflexive: for all $X \in \mathcal{C}$, $X \preceq X$.
- It is antisymmetric: for all $X, Y \in \mathcal{C}$, $X \preceq Y \preceq X$ implies $X = Y$.
- It is transitive: for all $X, Y, Z \in \mathcal{C}$, $X \preceq Y \preceq Z$ implies $X \preceq Z$.
- And, it is locally finite: for all $X, Y \in \mathcal{C}$, $|I(X, Y)| < \infty$, where $|\cdot|$ denotes cardinality and $I(X, Y)$ is the causal interval defined by $I(X, Y) := \{Z \in \mathcal{C} | X \preceq Z \preceq Y\}$.

The causal structure of a Lorentzian manifold already includes much of the information about the manifold. The metric, for example in a globally hyperbolic spacetime, is fully determined up to a conformal factor. The missing information is provided by a volume measure, which would fix the conformal factor. In a causal set, in addition to the causal structure we also have a measure of volume, set by the number of elements in the causal set. This is due to the final condition above, where we have a finite number of points in the causal set (in contrast to the continuum).

To produce a causal set $\mathcal{C}_\mathcal{M}$ that is the discrete underpinning of (or approximation to, depending on the point of view) a given continuous spacetime $\mathcal{M}$, we *sprinkle* points into $\mathcal{M}$. A sprinkling generates a causal set from a given Lorentzian manifold by placing points at random in $\mathcal{M}$ via a Poisson process with "density" ρ, such that the probability of having N points in a region of spacetime volume V is $P(N) = \frac{(\rho V)^N}{N!} e^{-\rho V}$. This produces a causal set whose elements are the sprinkled points and whose partial order relation is that of the manifold's causal relation restricted to the sprinkled points. The expected total number of elements in the causal set will be $N = \rho V_\mathcal{M}$. A causal set generated by sprinkling provides a discretisation of $\mathcal{M}$ which, unlike a regular lattice, is Lorentz invariant [5].

A causal set formed by sprinkling 500 elements into a finite interval in 1+1 Minkowski space, with a density $\rho = 1$, is shown in (figure 2.1).

A useful way to represent a causal set, is through an adjacency matrix. We will often use *causal matrices* in our causal set calculations. Let $\mathcal{C}$ contain p elements which we label $n_1, n_2, ...n_p$. The *causal matrix* is defined by

$$A_{xy} := \begin{cases} 1, & \text{if } n_x \prec n_y. \\ 0, & \text{otherwise} \end{cases} \tag{2.1}$$

The diagonal elements are set to zero. For example, if our causal set is:

$$C = \{n_1, n_2, n_3, n_4\} \tag{2.2}$$

where

$$\begin{aligned} &n_1 \preceq n_1, n_1 \preceq n_2, n_1 \preceq n_3, n_1 \preceq n_4 \\ &n_2 \preceq n_2, n_2 \preceq n_3 \\ &n_3 \preceq n_3 \\ &n_4 \preceq n_4 \end{aligned} \tag{2.3}$$

its causal matrix would be;

$$A = \begin{pmatrix} 0 & 1 & 1 & 1 \\ 0 & 0 & 1 & 0 \\ 0 & 0 & 0 & 0 \\ 0 & 0 & 0 & 0 \end{pmatrix}$$

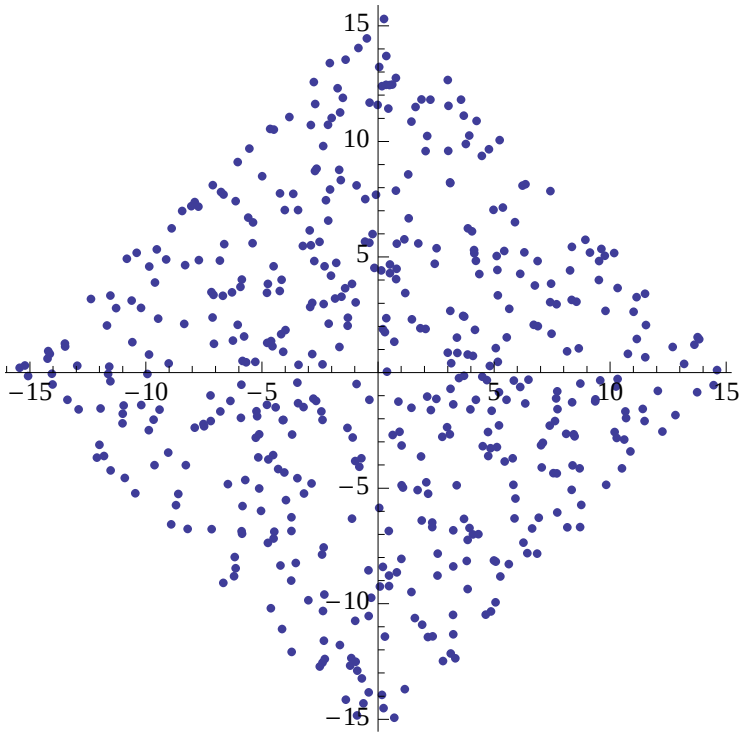

Figure 2.1: A causal set formed by sprinkling 500 elements into a finite interval in 1+1 Minkowski space, with a density $\rho = 1$.

Causal matrices are especially useful for constructing the propagators of the theory. The causal set retarded Green function for sprinklings into 1+1 Minkowski spacetime with a signature of $(+-)$, which we will be concerned with, is given by [27]:

$$K_R := \frac{1}{2} A \left(I + \frac{m^2}{2\rho} A \right)^{-1} \tag{2.4}$$

where I is the identity matrix. For more details on causal set theory the reader may refer to [7, 40, 24].

Chapter 3

The Sorkin-Johnston Vacuum

A large portion of this chapter appears in [2].

3.1 The SJ vacuum

We state the SJ proposal for the "ground state" of a free scalar field in a d-dimensional globally hyperbolic spacetime $(\mathcal{M}, g_{\mu\nu})$ [42, 26]. The starting point is the Pauli-Jordan function $\Delta(X, X')$, where we use capital letters X, X' to denote spacetime points. It is defined by

$$\Delta(X, X') := G_R(X, X') - G_R(X', X) \tag{3.1}$$

where G_R is the retarded propagator, i.e. the Green function of the Klein-Gordon operator[1] $\Box - m^2$ satisfying the retarded boundary condition, $G_R(X, X') = 0$ unless $X' \prec X$, meaning that X' is to the causal past of X. Notice that Δ is real and antisymmetric.

The rules of canonical quantisation relate the Pauli-Jordan function to the commutator of field operators by:

$$i\Delta(X, X') = [\hat{\phi}(X), \hat{\phi}(X')] \ , \tag{3.2}$$

while the Wightman two-point function of a state $|0\rangle$ is

$$W_0(X, X') = \langle 0|\hat{\phi}(X)\hat{\phi}(X')|0\rangle \ . \tag{3.3}$$

The Wightman function of the SJ state is defined by the three conditions [42]:

[1] The signature of the spacetime metric in this chapter is $(-+++\cdots+)$ and $\Box = g^{\mu\nu}\nabla_\mu\nabla_\nu$.

1. *commutator:* $i\Delta(X,X') = W(X,X') - W^*(X,X')$
2. *positivity:* $\int_{\mathcal{M}} dV \int_{\mathcal{M}} dV' f^*(X) W(X,X') f(X') \geq 0$
3. *orthogonal supports:* $\int_{\mathcal{M}} dV'\, W(X,X')\, W(X',X'')^* = 0,$

where $\int dV = \int d^dX \sqrt{-g(X)}$. On this view the Wightman function is a positive bilinear form on the vector space of complex functions. The first two conditions must be satisfied by the two-point function of any state. It is the third and last requirement that acts as the "ground state condition."

For the conditions to specify a state fully, their solution must be unique. Suppose W_1 and W_2 both satisfy the conditions. Let us express the ground state condition as $WW^* = 0$[2]. We have $W_1 W_1^* = W_1^* W_1 = W_2 W_2^* = W_2^* W_2 = 0$ and $W_1 - W_1^* = W_2 - W_2^*$. This implies

$$\begin{aligned} (W_1 - W_1^*)^2 &= (W_2 - W_2^*)^2 \\ \Rightarrow (W_1 + W_1^*)^2 &= (W_2 + W_2^*)^2 \,. \end{aligned}$$

Both $W_1 + W_1^*$ and $W_2 + W_2^*$ are positive bilinear forms, and if there are unique positive square roots of such forms then this implies

$$\begin{aligned} W_1 + W_1^* &= W_2 + W_2^* \\ \Rightarrow \quad W_1 &= W_2 \,. \end{aligned}$$

Formally, we can interpret the ground state condition as the requirement that W be the positive part of $i\Delta$, thought of as an operator on the Hilbert space of square integrable functions $L^2(\mathcal{M}, dV)$ [42]. This allows us to describe a more or less direct construction of W from the Pauli-Jordan function [26, 27, 30]. The distribution $i\Delta(X,X')$ defines the kernel of a (Hermitian) integral operator (which we may call the *Pauli-Jordan operator* $i\Delta$) on $L^2(\mathcal{M}, dV)$. The inner product on this space is

$$\langle f, g \rangle := \int_{\mathcal{M}} dV\, f(X)^* g(X), \tag{3.4}$$

where $dV = \sqrt{-g(X)} d^dX$ is the invariant volume-element on $\mathcal{M}$. The action of $i\Delta : f \mapsto i\Delta f$ is then given by

$$(i\Delta f)(X) := \int_{\mathcal{M}} dV' i\Delta(X,X') f(X'). \tag{3.5}$$

[2]Strictly speaking, to multiply two quadratic forms together requires a metric, here given by a delta function. In these formulas the star denotes numerical complex-conjugate, not hermitian adjoint.

When this operator is self-adjoint, it admits a unique spectral decomposition. Whether or not this (or some suitable generalization of it) is the case depends on the functional form of the kernel $i\Delta(X, X')$ and on the geometry of $\mathcal{M}$. For the massless scalar field on a bounded region of Minkowski space, such as the finite causal diamond which is the subject of this chapter, $i\Delta$ is indeed a self-adjoint operator, since the kernel $i\Delta(X, X')$ is Hermitian and bounded (see (3.28) below). In the following we assume that we can expand $i\Delta$ in terms of its eigenfunctions.

Noting that the kernel $i\Delta$ is skew-symmetric, we find that the eigenfunctions in the image of $i\Delta$ come in complex conjugate pairs T_q^+ and T_q^- with real eigenvalues $\pm\lambda_q$:

$$(i\Delta T_q^\pm)(X) = \pm\lambda_q T_q^\pm(X), \tag{3.6}$$

where $T_q^-(X) = [T_q^+(X)]^*$ and $\lambda_q > 0$. Now by the definition of $i\Delta$, these eigenfunctions must be solutions to the homogeneous Klein-Gordon equation. If they are L^2-normalised so that $||T_q^+||^2 := \langle T_q^+, T_q^+\rangle = 1$,[3] then the spectral decomposition of the Pauli-Jordan function implies that the kernel can be written as

$$i\Delta(X, X') = \sum_q \lambda_q T_q^+(X) T_q^+(X')^* - \sum_q \lambda_q T_q^-(X) T_q^-(X')^\star. \tag{3.7}$$

We now construct the SJ two-point function $W_{SJ}(X, X')$ by restricting (3.7) to its positive part:

$$W_{SJ}(X, X') := \sum_q \lambda_q T_q^+(X) T_q^+(X')^\star = \sum_q \mathcal{T}_q(X)\mathcal{T}_q(X')^\star \tag{3.8}$$

where $\mathcal{T}_q(X) := T_q^+(X)\sqrt{\lambda_q}$.

Let us compare this with the familiar case of the vacuum state of a free scalar field when the spacetime admits a timelike Killing vector $\kappa = \partial_t$. The free field can be expanded in a basis of modes, $\{u_k, u_k^*\}$, which are positive and negative frequency with respect to κ:

$$u_k(X) = u_k(t, \mathbf{X}) = N_k e^{-i\omega_k t} U_k(\mathbf{X})\,, \tag{3.9}$$

where N_k is a normalisation-factor, $\omega_k > 0$, and $\mathbf{X}$ are the spatial coordinates of X. When the emission and absorption operators that serve as the expansion coefficients are given their customary normalisation, then the Pauli-Jordan function can be expressed as a mode sum

$$i\Delta(X, X') = \sum_k \left[u_k(X)u_k^*(X') - u_k^*(X)u_k(X')\right]\,. \tag{3.10}$$

[3] When the spacetime region is non-compact this should be replaced by a delta-function normalisation $\langle T_q^+, T_{q'}^+\rangle = \delta(q - q')$.

The vacuum state corresponding to the choice of positive frequency modes u_k is the ground state of the Hamiltonian associated to κ, and its Wightman function is

$$W(X, X') = \sum_k u_k(X) u_k^*(X') \,. \tag{3.11}$$

Comparing (3.11) with (3.8) we see the eigenfunctions $\mathcal{T}_q := \sqrt{\lambda_q} T_q^+$ chosen by the SJ condition are the analogues of the positive frequency modes in the static spacetime, but the SJ construction does not require the existence of a timelike isometry.

When there *is* a timelike Killing vector, we can show that the SJ state (formally extended to the case of a spacetime of infinite volume) is the ground state of the Hamiltonian associated with that Killing vector by showing that the Wightman function defined by (3.11) satisfies the SJ conditions. Clearly, (3.11) satisfies conditions (i) and (ii), and it only remains to check the ground state condition (iii). We have

$$\begin{aligned}
WW^*(X, X'') &= \int_{\mathcal{M}} dV' W(X, X') W^*(X', X'') \\
&= \sum_k \sum_l u_k(X) u_l(X'') \int dt d^{n-1}\mathbf{X}' \sqrt{-g(X')} u_k^*(X') u_l^*(X') \\
&= \sum_k \sum_l u_k(X) u_l(X'') \int d^{n-1}\mathbf{X}' \sqrt{-g(\mathbf{X}')} U_k^*(\mathbf{X}') U_l^*(\mathbf{X}') \int_{-\infty}^{\infty} dt e^{-i\omega_k t} e^{-i\omega_l t} \\
&= \sum_k \sum_l u_k(X) u_l(X'') \int d^{n-1}\mathbf{X}' \sqrt{-g(\mathbf{X}')} U_k^*(\mathbf{X}') U_l^*(\mathbf{X}') \int_{-\infty}^{\infty} dt e^{-i(\omega_k + \omega_l) t} \\
&\propto \delta(\omega_k + \omega_l) = 0
\end{aligned}$$

since the sum over modes does not include the zero-mode $\omega_k = 0$. Thus, if the globally timelike Killing vector admits a unique ground state, the SJ conditions also specify a unique state which agrees with that state.

This might be a good place to comment on the question of whether the SJ vacuum obeys the so-called Hadamard condition [29, 14] on its short-distance behavior. In static spacetimes the Hamiltonian vacuum obeys this condition, so the SJ vacuum does as well, as we have just seen. On the other hand, Fewster and Verch [19] have recently provided examples of regions where the condition does not hold. In our opinion, the significance of the Hadamard condition will not be known until we understand better the nature of quantum gravity and its semiclassical approximations. Outside of that context Hadamard behavior seems irrelevant "operationally", since it corresponds in the Wightman function to the absence of a term that could only be noticed at extremely high energies. We hope

to return to this question in another place, and to show in particular how, by "smoothing the boundary", one can tweak the ultraviolet behavior of the SJ state so that it becomes Hadamard.

3.2 The massless scalar field in two-dimensional flat spacetimes

As background for our investigation of the massless scalar field in a two-dimensional causal diamond, we review the massless scalar field in two-dimensional Minkowski and Rindler spacetimes. The metric on Minkowski spacetime in Cartesian coordinates (t, x) is given by

$$ds^2_M = -dt^2 + dx^2. \tag{3.12}$$

Since the spacetime is globally hyperbolic and static with timelike Killing vector $\kappa_M = \partial_t$, we can separate the solutions to the Klein-Gordon equation into positive and negative frequency with respect to κ_M. The field equation is

$$\Box_M \phi = -\partial_t^2 \phi + \partial_x^2 \phi = 0 \tag{3.13}$$

and the normalised positive frequency modes can be taken as

$$u_k^M(t, x) = \frac{1}{\sqrt{4\pi\omega_k}} e^{-i\omega_k t + ikx}, \tag{3.14}$$

where $\omega_k = |k|$.

These modes and their complex conjugates form a complete orthonormal basis with inner product

$$(u_{k1}, u_{k2}) = -i \int u_{k1}(t, x) \overset{\leftrightarrow}{\partial_t} u^*_{k2}(t, x) dx \tag{3.15}$$

where the integral is over a spacelike hyperplane of simultaneity at an instant t, and the modes (3.14) are normalized as

$$(u_k^M, u_{k'}^M) = \delta(k - k') \tag{3.16}$$

The field operator can be expanded in terms of the modes (3.14) as:

$$\hat{\phi}(t, x) = \int [\hat{a}_k u_k^M(t, x) + \hat{a}_k^\dagger u_k^{M*}(t, x)] dk \tag{3.17}$$

and the standard commutation relations hold:

$$[a_k, a_{k'}] = 0 \tag{3.18}$$
$$[a^\dagger{}_k, a^\dagger{}_{k'}] = 0 \tag{3.19}$$
$$[a_k, a^\dagger{}_{k'}] = \delta(k - k') \tag{3.20}$$

If we try to define a vacuum state, $|0_M\rangle$ in the usual way as the state annihilated by the operator coefficients of the positive frequency modes in the expansion of the field operator $\hat{\phi}(t, x)$, then it is well-known that we encounter an infrared divergence [11, 1, 18]:

$$\begin{aligned} W_M(t, x; t', x') &:= \langle 0_M | \hat{\phi}(t, x) \hat{\phi}(t', x') | 0_M \rangle \\ &= \frac{1}{4\pi} \int_{-\infty}^{\infty} \frac{dk}{|k|} e^{-i|k|(t-t')+ik(x-x')}, \end{aligned} \tag{3.21}$$

which is logarithmically divergent at $k = 0$.

Following [1], we can remove the divergence by introducing an infrared momentum cutoff λ

$$\begin{aligned} &\frac{1}{4\pi} \int_{-\infty}^{\infty} \frac{dk}{|k|} e^{-i|k|\Delta t + ik\Delta x} \theta(|k| - \lambda) \\ &= \frac{1}{4\pi} \lim_{\epsilon \to 0^+} \int_{\lambda}^{\infty} \frac{dk}{k} \left[e^{-ik(\Delta t + \Delta x - i\epsilon)} + e^{-ik(\Delta t - \Delta x - i\epsilon)} \right] \\ &= -\frac{1}{4\pi} \lim_{\epsilon \to 0^+} \left[\ln \left[i(\Delta t + \Delta x - i\epsilon)\mu \right] + \ln \left[i(\Delta t - \Delta x - i\epsilon)\mu \right] \right] + \mathcal{O}(\lambda\Delta) \\ &= -\frac{1}{2\pi} \ln \mu |d| - \frac{i}{4} \mathrm{sgn}(\Delta t) \theta(\Delta t^2 - \Delta x^2) + \mathcal{O}(\lambda\Delta), \end{aligned} \tag{3.22}$$

where $\mu = \lambda e^\gamma$, γ is the Euler-Mascheroni constant, and $\Delta t = t - t'$, $\Delta x = x - x'$, and $d = \sqrt{-\Delta t^2 + \Delta x^2}$. The logarithm here is given a branch cut on the negative real axis and ln denotes its principal value. The quantity Δ here stands collectively for Δt and Δx, such that small $\lambda\Delta$ implies that both coordinate distances Δt and Δx are small compared to λ^{-1}. With non-zero λ, the theory has a preferred frame. However, if we drop the $\mathcal{O}(\lambda)$ term in (3.22), we obtain a one-parameter family of two-point functions that depend on λ but are fully frame-independent (in the sense that their real part only depends on d):

$$W_{M,\lambda}(t, x; t', x') := -\frac{1}{2\pi} \ln \mu |d| - \frac{i}{4} \mathrm{sgn}(\Delta t) \theta(\Delta t^2 - \Delta x^2) \tag{3.23}$$

Unfortunately, (3.23) cannot itself serve as a physical Wightman function, because it fails to be positive as a quadratic form (this being condition (ii) above). Nevertheless we will see that the form (3.23) will emerge in a natural manner as a certain limit of the two-point function we will derive for the diamond.[4]

It is worth noting that the theory whose fundamental field is the gradient of ϕ rather than ϕ itself is not infrared divergent, and in fact the vacuum expectation value

$$\langle 0_M|\nabla_\mu\hat{\phi}(t,x)\hat{\phi}(t',x')|0_M\rangle = \frac{\Delta x_\mu}{2\pi(\Delta t^2 - \Delta x^2)} \tag{3.24}$$

already converges, except for the singularity on the lightcone.

The Rindler metric [33, 34] arises from the Minkowski metric via the coordinate transformations $t = a^{-1}e^{a\xi}\sinh a\eta$ and $x = a^{-1}e^{a\xi}\cosh a\eta$, where $a > 0$ is a constant with dimensions of inverse length and $-\infty < \xi, \eta < \infty$. The coordinates ξ and η only cover a submanifold of the full Minkowski space, namely the right Rindler wedge, $x > |t|$; but this submanifold is conformal to all of Minkowski space as one sees from the form of the line element in ξ-η coordinates:

$$ds_R^2 = e^{2a\xi}\left(-d\eta^2 + d\xi^2\right). \tag{3.25}$$

Lines of constant ξ are hyperbolae that correspond to the trajectories of observers accelerating eternally at a constant acceleration $ae^{-a\xi}$ (figure 3.1), and are integral curves of the Killing vector $\kappa_R = \partial_\eta$.

Since Rindler spacetime is globally hyperbolic and static in its own right, the canonical quantisation of the scalar field can be carried out in a completely self-contained manner [21]. Thanks to the conformal invariance of the massless theory in two dimensions, the field equation $\Box_R\phi = 0$ in Rindler coordinates (3.25) is just the usual wave equation, whose normalised positive frequency solutions, the Fulling-Rindler modes, are given by the plane waves

$$u_p^R = \frac{1}{\sqrt{4\pi\omega_p}}e^{-i\omega_p\eta + ip\xi}\ , \tag{3.26}$$

where $\omega_p = |p|$. Trying to define a Fulling-Rindler vacuum state $|0_R\rangle$ as the state annihilated by the operator coefficients of the positive frequency Rindler modes in the expansion of $\hat{\phi}$ once again results in an infrared divergent integral for the two-point function W. Proceeding as before, one can introduce a cutoff at small "momentum" λ and discard a term

[4] Perhaps (3.23) could also be understood as defining an "approximate state" valid when Δt and Δx are small compared to the IR scale λ^{-1}.

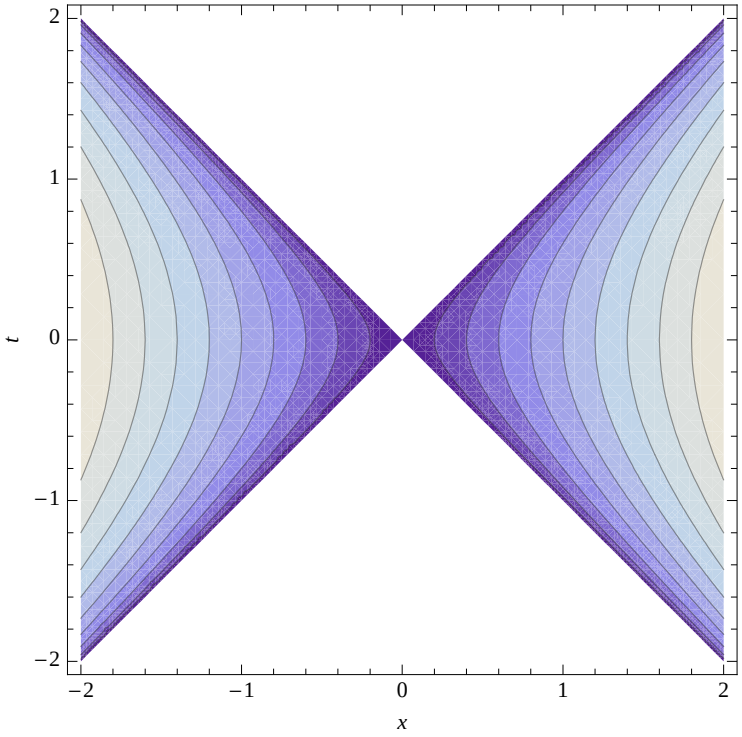

Figure 3.1: The right and left Rindler wedges of two-dimensional Minkowski spacetime.

of order λ to obtain a one-parameter family of two-point functions, which are the same functions of Rindler coordinates as the Minkowski two-point function (3.23) is of Cartesian coordinates:

$$W_{R,\lambda}(\eta,\xi;\eta',\xi') \;:=\; -\frac{1}{4\pi}\ln\mu^2|\Delta\eta^2-\Delta\xi^2| - \frac{i}{4}\mathrm{sgn}(\Delta\eta)\theta(\Delta\eta^2-\Delta\xi^2) \qquad (3.27)$$

where $\mu=\lambda e^{\gamma}$. As before, this two-point function is symmetric (boost-invariant) but fails to be positive and depends explicitly on the cutoff λ. At best it can have an approximate validity when the coordinate-differences $\Delta\eta$ and $\Delta\xi$ are small compared to λ^{-1}.

It is well known that the Minkowski and Fulling-Rindler "ground states" corresponding to (3.23) and (3.27) are not equal, since the Rindler mode functions u_k^R are linear combinations of both positive and negative frequency Minkowski mode functions u_k^M and u_k^{M*}. This phenomenon is by now well understood as an instance of the Fulling-Davies-Unruh effect [21, 12, 46]: if the Rindler wedge is understood as a subregion of Minkowski space, and the field is in the usual Poincaré-invariant vacuum state (say in $3+1$ dimensions, where

the latter is well defined), observers that are confined to the wedge and that accelerate eternally at a uniform rate will feel themselves immersed in a thermal bath of particles.

The preceding calculations suffer from the appearance of infinite integrals and the consequent need for infrared cutoffs. Nevertheless, we will see that the two-point functions we have obtained in this section can be related to the case we study next, that of a *finite* two-dimensional causal diamond, where the the SJ construction and the integrals it gives rise to are completely well-defined. In this connection we comment also that inasmuch as both the Minkowski and Rindler spacetimes possess globally timelike Killing vectors, the formal demonstration of section 3.1 would apply to show that the SJ vacua of these two spacetimes would coincide with the ground-states discussed in this section – were such states actually to exist. (See also [30].)

3.3 The massless SJ two-point function in the flat causal diamond

A causal diamond (or Alexandrov open set) is the intersection of the chronological future of a point p with the chronological past of a point $q \succ p$. Because such a causal diamond is a globally hyperbolic manifold in its own right, the scalar field possesses therein a unique Pauli-Jordan function Δ. In this section we will follow the SJ procedure to derive from Δ a two-point function W for the massless scalar field in a causal diamond in two-dimensional Minkowski space. We will then analyse the limit of W for points (i) in the centre of the diamond and (ii) in the corner of the diamond.

Lightcone coordinates $u = (t+x)/\sqrt{2}$ and $v = (t-x)/\sqrt{2}$ are most convenient in this section. A causal diamond centred at the origin $u = v = 0$ that corresponds to the region $u, v \in (-L, L)$ is shown in figure 3.2 and will be denoted by C_L. Its spacetime volume is $V = 4L^2$. The commutator function $i\Delta(X, X')$ can be calculated in lightcone coordinates from the retarded and advanced propagators [4]:

$$i\Delta(u, v; u', v') = -\frac{i}{2}[\theta(u-u') + \theta(v-v') - 1] \ . \tag{3.28}$$

Given that C_L is a bounded region of spacetime, the associated integral operator $i\Delta$ defined in (3.5) is of *Hilbert-Schmidt* type, i.e. its Hilbert-Schmidt norm is finite:

$$\int_{-L}^{L} du \int_{-L}^{L} dv \int_{-L}^{L} du' \int_{-L}^{L} dv' |i\Delta(u, v; u', v')|^2 = 2L^4 < \infty. \tag{3.29}$$

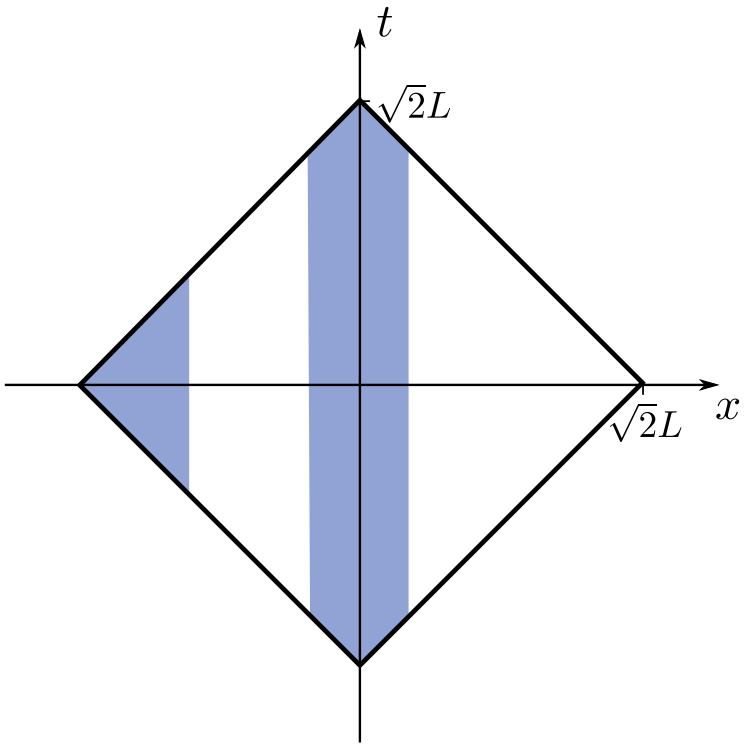

Figure 3.2: The causal diamond, $u, v \in (-L, L)$. The shaded portions of the diagram represent the centre (i) and corner (ii) regions of interest in section 3.3.

Since $i\Delta(X, X') = [i\Delta(X', X)]^*$, $i\Delta$ is also self-adjoint and so the spectral theorem applies. The positive eigenfunctions T_k^+ that satisfy $i\Delta T_k^+ = +\lambda_k T_k^+$, are given by the two sets [27]

$$f_k(u, v) := e^{-iku} - e^{-ikv}, \qquad \text{with } k = \frac{n\pi}{L},\ n = 1, 2, \ldots \tag{3.30}$$

$$g_k(u, v) := e^{-iku} + e^{-ikv} - 2\cos(kL), \qquad \text{with } k \in \mathcal{K}, \tag{3.31}$$

where $\mathcal{K} = \{k \in \mathbb{R} \mid \tan(kL) = 2kL \text{ and } k > 0\}$ and their eigenvalues are $\lambda_k = L/k$.[5] Their L^2-norms are $||f_k||^2 = 8L^2$ and $||g_k||^2 = 8L^2 - 16L^2\cos^2(kL)$. It is clear that the eigenfunctions T_k^- with negative eigenvalues are given by the complex conjugates $T_k^- = [T_k^+]^*$. To verify that the functions (3.30-3.31) and their complex conjugates are indeed *all* the eigenfunctions with non-zero eigenvalue, we can use the fact [27, 45] that the sum over the

[5]There is a sign error in the commutator function in [27] which results in the f_k and g_k given here being the complex conjugates of those there.

squared eigenvalues of a Hilbert-Schmidt operator is equal to its Hilbert-Schmidt norm. A short calculation shows that

$$\sum_k \lambda_k^2 = \sum_{n=1}^{\infty} \frac{2L^4}{(\pi n)^2} + \sum_{k\in\mathcal{K}} \frac{2L^2}{k^2} = \frac{2L^4}{6} + \frac{10L^4}{6} = 2L^4 \tag{3.32}$$

coincides with (3.29), as required (the analytic evaluation of the second sum in (3.32) can be found in [27, 44]). The SJ prescription defines the two-point function $W_{SJ,L}(u,v;u',v')$ as the positive spectral projection of $i\Delta$:

$$W_{SJ,L}(u,v;u',v') = \sum_{n=1}^{\infty} \frac{L^2}{\pi n} \frac{1}{||f_k||^2} f_k(u,v) f_k^*(u',v') + \sum_{k\in\mathcal{K}} \frac{L}{k} \frac{1}{||g_k||^2} g_k(u,v) g_k^*(u',v'). \tag{3.33}$$

We denote the two sums in (3.33) by S_1 and S_2, respectively.
The first sum

$$S_1 = \frac{1}{8\pi} \sum_{n=1}^{\infty} \frac{1}{n} \left[e^{-\frac{iun\pi}{L}} - e^{-\frac{ivn\pi}{L}} \right] \left[e^{\frac{iu'n\pi}{L}} - e^{\frac{iv'n\pi}{L}} \right] \tag{3.34}$$

can be evaluated in closed form. We recognize four Newton-Mercator series which converge to the principal branch of the complex logarithm:

$$\begin{aligned} S_1 = \frac{1}{8\pi} \Big\{ &-\ln\left[1 - e^{-\frac{i\pi(u-u')}{L}}\right] - \ln\left[1 - e^{-\frac{i\pi(v-v')}{L}}\right] \\ &+\ln\left[1 - e^{-\frac{i\pi(u-v')}{L}}\right] + \ln\left[1 - e^{-\frac{i\pi(v-u')}{L}}\right] \Big\}. \end{aligned} \tag{3.35}$$

The second sum is

$$S_2 := \sum_{k\in\mathcal{K}} \frac{\left[e^{-iku} + e^{-ikv} - 2\cos(kL)\right]\left[e^{iku'} + e^{ikv'} - 2\cos(kL)\right]}{kL\left[8 - 16\cos^2(kL)\right]}. \tag{3.36}$$

We have no closed form expression for this sum but as $n \to \infty$, the roots of the transcendental equation $\tan(x) = 2x$ rapidly approach $x_n = \frac{(2n-1)\pi}{2}$ with $n \in \mathbb{N}$ (see figure 3.3). Therefore if we approximate the sum by replacing $k \in \mathcal{K}$ with x_n/L, we can expect the main error to come from a few modes of long wavelength. Consequently we can expect the resulting error term to be a slowly varying and small correction to the approximated sum.

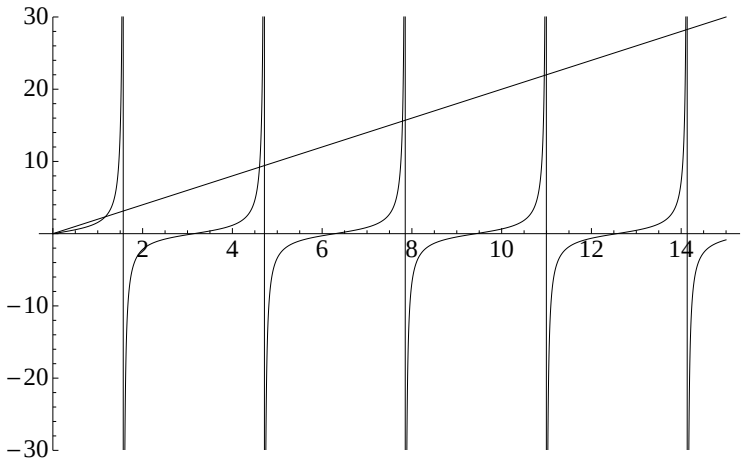

Figure 3.3: Plot of $\tan x$ and $2x$ along with vertical lines at $\frac{2n-1}{2}\pi$ for $n \in \mathbb{Z}$. The values of the summation variable are the positions of the intersections $\tan x = 2x > 0$.

Let $\mathcal{K}_0 := \left\{ \frac{2n-1}{2L}\pi \,|\, n = 1, 2, 3 \ldots \right\}$ and define the error $\epsilon(u, v; u', v')$ by

$$\begin{aligned} S_2 =& \sum_{k \in \mathcal{K}_0} \frac{\left[e^{-iku} + e^{-ikv} - 2\cos(kL)\right]\left[e^{iku'} + e^{ikv'} - 2\cos(kL)\right]}{kL\left[8 - 16\cos^2(kL)\right]} + \epsilon(u, v; u', v') \\ =& \frac{1}{4\pi} \sum_{n=1}^{\infty} \frac{1}{2n-1} \left[e^{-\frac{iu(2n-1)\pi}{2L}} + e^{-\frac{iv(2n-1)\pi}{2L}}\right]\left[e^{\frac{iu'(2n-1)\pi}{2L}} + e^{\frac{iv'(2n-1)\pi}{2L}}\right] + \epsilon(u, v; u', v') \,. \end{aligned} \tag{3.37}$$

The sums above converge to logarithmic terms when $L < \infty$ and are most conveniently expressed in the form:

$$\begin{aligned} S_2 = \frac{1}{4\pi} \Big\{ &\tanh^{-1}\left[e^{-\frac{i\pi(u-u')}{2L}}\right] + \tanh^{-1}\left[e^{-\frac{i\pi(v-v')}{2L}}\right] \\ &+ \tanh^{-1}\left[e^{-\frac{i\pi(u-v')}{2L}}\right] + \tanh^{-1}\left[e^{-\frac{i\pi(v-u')}{2L}}\right] \Big\} + \epsilon(u, v; u', v') \end{aligned} \tag{3.38}$$

The two-point function of the SJ ground state in the causal diamond is given by the sum, $W_{SJ,L} = S_1 + S_2$. Using $\tanh^{-1}(x) = \frac{1}{2}\ln(1+x) - \frac{1}{2}\ln(1-x)$ and the fact that

$\ln(1-e^x) - \ln(1+e^{\frac{x}{2}}) = \ln(1-e^{\frac{x}{2}})$, we can combine the two sums to yield

$$\begin{aligned} W_{SJ,L} = \frac{1}{4\pi}\Big\{ &-\ln\left[1-e^{-\frac{i\pi(u-u')}{2L}}\right] - \ln\left[1-e^{-\frac{i\pi(v-v')}{2L}}\right] \\ &+\ln\left[1-e^{-\frac{i\pi(u-v')}{2L}}\right] + \ln\left[1-e^{-\frac{i\pi(v-u')}{2L}}\right]\Big\} + \epsilon(u,v;u',v') \\ = W_{\text{box},L} &+ \epsilon(u,v;u',v'), \end{aligned} \tag{3.39}$$

where $W_{\text{box},L}$ is the exact continuum two-point function of the *ground state* of a massless scalar field in a box with reflecting boundaries at $x = \pm\sqrt{2}L$. We shall now investigate the form of the SJ ground state in the limits (i) and (ii) mentioned above.

The SJ state in the centre and corner

The limits we are concerned with require that two spacetime points be separated by a small geodesic distance compared to the diamond scale L and that they be confined to (i) the centre of the diamond or (ii) a region near the left/right corner (we choose the left corner without loss of generality). In these particular limits, we want the arguments in the exponentials of the sums above to have a small magnitude so that we can Taylor expand the functions and obtain more illuminating forms of the two-point function. Keeping in mind that in u, v-coordinates, the centre of the diamond lies at $(0,0)$, the limit that corresponds to a pair of points in the centre (i) can be defined as

$$|u-u'| \ll L \quad , \qquad |v-v'| \ll L, \qquad |u-v'| \ll L, \qquad |v-u'| \ll L. \tag{3.40}$$

The limit that corresponds to the corner can be obtained in a similar manner by first translating the coordinate system such that the left corner of the diamond lies at the origin $(0,0)$ of the new coordinates. This corresponds to the (passive) coordinate transformation $x \to x - \sqrt{2}L$, or $u \to u - L$ and $v \to v + L$. By "in the corner" we then mean the limit (ii) where we first perform this translation and then apply the restriction (3.40) to the translated coordinates.

The inequalities (3.40) constrain the pairs of spacetime points to be separated by a small geodesic distance $|d| = (2|u-u'||v-v'|)^{\frac{1}{2}} \ll L$ and furthermore imply that $|x|, |x'| \ll L$. This means that the points are confined to a narrow vertical strip centred on (i) the centre of the diamond or (ii) the left corner of the diamond, as illustrated in figure 3.2. Let the width of the strip be $D \ll L$.

The centre

We first analyse the sum in the centre by expanding to lowest order in δ/L, where δ collectively denotes the coordinate differences $u-u', v-v', u-v', v-u'$. Using $\ln(1-e^x) = \ln(x) + \mathcal{O}(x)$ we identify the leading term in S_1 as

$$S_1 = \frac{1}{8\pi}\left[-\ln|u-u'||v-v'| + \ln|u-v'||v-u'| + C_1\frac{i\pi}{2}\right] + \mathcal{O}\left(\frac{\delta}{L}\right) \tag{3.41}$$

where $C_1 = \mathrm{sgn}(u-u') + \mathrm{sgn}(v-v') - \mathrm{sgn}(u-v') - \mathrm{sgn}(v-u')$. Similarly, in S_2, we expand $\tanh^{-1}(e^x) = -\frac{1}{2}\ln\frac{x}{2} + \mathcal{O}(x)$ to obtain

$$S_2 = \frac{1}{8\pi}\left[-\ln|u-u'||v-v'| - \ln|u-v'||v-u'| - 4\ln\frac{\pi}{4L} + C_2\frac{i\pi}{2}\right] + \epsilon + \mathcal{O}\left(\frac{\delta}{L}\right), \tag{3.42}$$

where $C_2 = \mathrm{sgn}(u-u') + \mathrm{sgn}(v-v') + \mathrm{sgn}(u-v') + \mathrm{sgn}(v-u')$.

Now we deal with the correction, ϵ. Over a small region, ϵ should not vary much. To investigate this, we now further restrict the arguments of W to lie in a small square centred on the origin, of linear dimension D, the width of the strip. After an analysis and numerical investigation given in the appendix, we find that ϵ is indeed approximately constant over the small diamond and tends to a value $\epsilon_{\text{centre}} \approx -0.063$ as L tends to infinity.

The terms with arguments $u-v'$ and $v-u'$ cancel in S_1+S_2 so we obtain:

$$W_{\text{centre}}(u,v;u',v') = -\frac{1}{4\pi}\ln|\Delta u\Delta v| - \frac{i}{4}\mathrm{sgn}(\Delta u+\Delta v)\theta(\Delta u\Delta v) - \frac{1}{2\pi}\ln\frac{\pi}{4L} + \epsilon_{\text{centre}} + \mathcal{O}\left(\frac{\delta}{L}\right), \tag{3.43}$$

as L gets large. Recall now that $|\Delta u\Delta v| = \frac{1}{2}|d|^2$. It is then evident that (3.43) matches the "cut off" Minkowski two-point function $W_{M,\lambda}$ (3.23) with a particular value of the cutoff λ given by

$$\lambda = \frac{\pi}{4\sqrt{2}}\exp(-\gamma - 2\pi\epsilon_{\text{centre}})L^{-1} \approx 0.46 \times L^{-1}\ , \tag{3.44}$$

where γ is the Euler-Mascheroni constant.

As one would expect, $\lambda^{-1} \sim L$ for large L, leading to a logarithmic factor of the form $\ln|L^2/\Delta u\Delta v|$.

Whilst strictly speaking we cannot take the $L\to\infty$ limit of such an expression, it seems fair to say that the SJ state takes on the character of a Minkowski vacuum in the centre

of a large diamond. (One might wonder how this is possible given that the regularized Minkowski vacuum violates positivity but the SJ state does not. It is possible that the discrepancy is to be found in the last term of (3.43), and in any case, as already mentioned, we cannot really take the limit $L \to \infty$). Notice finally that, for any L, the imaginary part of the two-point function does satisfy the requirement $\Im(W) = \Delta/2$, as had to be the case.

The corner

For spacetime points close to the edges of the diamond, the boundaries of the diamond appear like the causal horizons of a Rindler wedge (see figure 3.1). To evaluate the SJ two-point function in this limit, we perform the translation $u \to u - L$ and $v \to v + L$ described above, which shifts the corner of the diamond to the position $(0, 0)$. We then Taylor expand using (3.40) in the new coordinates.

The sums S_1 and S_2 can be evaluated as before, but the translation introduces $\pm$ signs multiplying integer multiples of $i\pi$. A brief inspection shows that the first sum (3.34) is unaltered by the translation, since only factors of $\exp(2\pi i)$ arise, while the second sum (3.36) picks up factors of $\exp(\pi i)$ that induce sign changes in the terms involving $u - v'$ and $v - u'$. The second sum now evaluates to

$$S_2 = \frac{1}{8\pi}\left[-\ln|u-u'||v-v'| + \ln|u-v'||v-u'| + C_2\frac{i\pi}{2}\right] + \epsilon + \mathcal{O}\left(\frac{\delta}{L}\right), \tag{3.45}$$

where $C_2 = \mathrm{sgn}(u-u') + \mathrm{sgn}(v-v') - \mathrm{sgn}(u-v') - \mathrm{sgn}(v-u') = C_1$. The correction term ϵ can again be analysed numerically — see appendix A — and the result is that it varies very little over the small corner region for fixed L and tends to zero as $L \to \infty$. A consequence of the sign changes is that the constant terms that depend on L cancel in S_2, whence there is no longer any obstruction sending $L \to \infty$. Taking this limit, we obtain the two-point function

$$\begin{aligned}\lim_{L\to\infty} W_{\text{corner}}(u,v;u',v') = &-\frac{1}{4\pi}\ln\left|\frac{(u-u')(v-v')}{(u-v')(v-u')}\right| \\ &-\frac{i}{4}\mathrm{sgn}(\Delta u + \Delta v)[\theta(\Delta u \Delta v) - \theta((v'-u)(u'-v))],\end{aligned} \tag{3.46}$$

which can be recognised as the two-point function of the scalar field in Minkowski space with a mirror at rest at the corner $x = 0$ ($x = -\sqrt{2}L$ in the original coordinates) [3, 13]:

$$W_{\text{corner}}(t,x;t',x') = W_{M,\lambda}(t,x;t',x') - W_{M,\lambda}(t,x;t',-x'). \tag{3.47}$$

This two-point function is scale-free and does *not* have the character of a canonical vacuum for a Rindler wedge.

What conclusions can we draw from this? Previously, we argued heuristically that the SJ state in the Rindler wedge should be the Fulling-Rindler vacuum (to the extent that either is defined at all in the presence of the IR divergences). Now we have seen that a well-controlled limiting procedure gives a different result. As L gets large, the spacetime geometry approaches that of the Rindler wedge, as far as points that remain close to one corner of the diamond are concerned, but the SJ state approaches the ground state of a scalar field with reflecting boundary conditions at the corner.

In fact, this "mirror behaviour" is already visible at the level of the SJ modes themselves. The first set of modes f_k (3.31) vanish on the two vertical lines at the spatial positions of the corners $f_k(x = \pm\sqrt{2}L, t) = 0$ (recall that the corners are at $x = \pm\sqrt{2}L$ in the coordinate system before translation), while the second set g_k also vanish on these vertical lines in the approximation $\mathcal{K} \to \mathcal{K}_0$. The SJ conditions thus satisfy approximately the boundary conditions for two static mirrors, one at each corner of the diamond. How would such a two-mirror state appear near to the left corner? As the size of the diamond tended to infinity, one might expect the field in the left corner to become unaware of the right mirror, and this is consistent with our calculation above. On the other hand there remains the puzzle of where the left-hand mirror comes from in the limit. Its very existence selects a distinguished timelike direction, and since this direction can only be covariantly defined by reference to the right hand corner of the diamond, it seems difficult to avoid the conclusion that the presence of the right corner retains its influence no matter how large L becomes!

It seems reasonable to attribute these counter-intuitive effects to our having set the mass to zero. As an aspect of its infrared pathology, the massless field might be able to sense the boundaries of the finite system, no matter how far away they are. If this explanation is correct, one would not expect to find the same mirror behavior for a massive scalar field, since the mass should shield it from such long range effects. It would also be interesting to study massless and massive fields in finite regions of Minkowski spacetime in $3 + 1$ dimensions.

3.3.1 Comparison with the discrete SJ vacuum

In this section, following [26, 27], we will apply the SJ formalism to the massless scalar field on a causal set that is well-approximated by the two-dimensional flat causal diamond. In the case of non-zero mass, the second of these references has shown numerically that

the mean of the discrete SJ two-point function approximates well the Wightman function of the continuum Minkowski vacuum.

The discrete version of the SJ prescription can be interpreted in two ways. In the context of quantum gravity, causal sets are considered to be fundamental — more fundamental than continuum spacetimes which are just approximations to the true discrete physics [7]. On this view, the discrete SJ proposal is a starting point for building a theory of quantum fields on the physical discrete substratum of spacetime and one can hope that it will give us clues about quantum gravity, just as quantum field theory in curved continuum spacetime has done. From another viewpoint, the discrete formalism can be seen as simply a Lorentz-invariant discretisation of the continuum formalism and can therefore be used to test or extend the results of the continuum theory, in particular when analytic calculations are difficult.

Causal sets and discrete propagators

In the remainder of this section, we will set $\rho = 1$ so that area will be measured directly by number of causet elements. Distance and area will thus be measured in *natural units*.

The discrete SJ two-point function for a scalar field on a finite causal set [27, 26] is constructed using the same procedure as described above: from the retarded Green function G_R, the Pauli-Jordan operator $i\Delta$ (a finite Hermitian matrix) is constructed and the Wightman function[6] w is then obtained as the positive part of $i\Delta$. In a finite causal set, this procedure is rigorously defined since everything is finite. It is of course necessary that the discrete analogue of the retarded Green function be known, which it is for massless [41] and massive [25] scalar fields on a sprinkling into two–dimensional Minkowski spacetime. The SJ two-point function is a complex-valued function of pairs of causal set elements, $w : \mathcal{C} \times \mathcal{C} \to \mathbb{C}$; equivalently it is a complex matrix $w^{ij} := w(\nu_i, \nu_j)$, where $\nu_i, \nu_j \in \mathcal{C}$. When $\mathcal{C}$ is obtained by sprinkling, each causal set element ν_i corresponds to a point X_i in the embedding continuum spacetime. This allows us to directly compare the values of the discrete two-point function w^{ij} and those of the continuum Wightman function $W^{ij} := W(X_i, X_j)$.

There is numerical evidence [26] for a massive scalar field that at high sprinkling density, the SJ two-point function in the causet approximates the known Minkowski-space Wightman function.

We will extend this study to the massless case and compare with our results above for the continuum SJ vacuum. We will compare the mean of the massless discrete two-point

[6] We use a lower case w for the causet counterpart of the continuum function W.

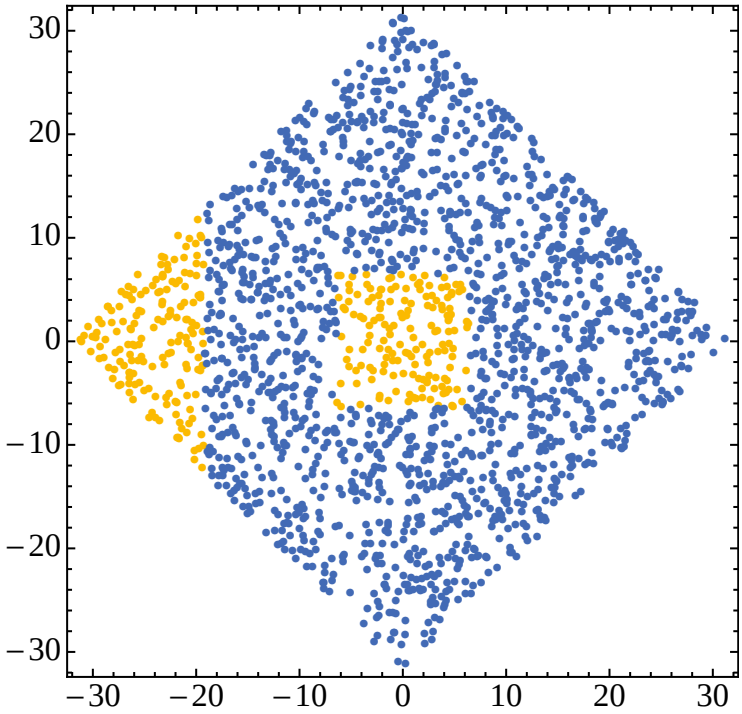

Figure 3.4: An $N = 2^{11} = 2048$ element sprinkling into a diamond C_L (with $L = 2^{\frac{9}{2}}$ in natural units). The subregions corresponding to the centre (i) and the corner (ii) are highlighted.

function w with its continuum counterparts, using two separate methods. In the centre of the diamond, the continuum two-point function (3.43) is approximately a function of the geodesic distance only, in the limit of large L. We therefore plot the amplitudes w^{ij} against the proper time $|d(X_i, X_j)|$ and ask how well they agree with the continuum result. In the corner, the continuum W does not reduce, to a function of a single variable. In that case, we provide a "correlation plot" between the discrete two-point function and several continuum two-point functions (evaluated on the sprinkled points), so that the relative goodness of fit can be assessed.

We restrict ourselves here to timelike related points; the analysis for spacelike related points is similar. Furthermore we only need to analyze the real parts of W and w. The imaginary parts add nothing new since they are given by the Pauli-Jordan function and tell us nothing about the quantum state.

We work in a causal diamond $\mathcal{M} = C_L$ and evaluate the discrete propagator on an $N = 2^{11} = 2048$ element sprinkling into this diamond, which implies $L = \sqrt{V}/2 = \sqrt{N}/2 = 2^{\frac{9}{2}}$ in natural units. A typical sprinkling is shown in figure 3.4. Highlighted are the two subregions in which we shall sample the discrete SJ two-point function. Each subregion occupies 8% of the area of the full diamond.

The SJ vacuum in the centre

The data for the centre is taken from a sample of 181 points in the square, among which there were 7599 timelike related pairs. As discussed in section 3 the two-point function of the massless scalar field in two–dimensional Minkowski spacetime is ill-defined owing to the infrared divergence, but there exists a one-dimensional family of "approximate Wightman functions" $W_{M,\lambda}$ parameterized by an infrared scale or "cutoff" λ. It is thus natural to compare our discrete function w with $W_{M,\lambda}$, where we fix $\lambda = 0.02$ from the relation (3.44) between λ and L when $L = 2^{\frac{9}{2}}$. Then the real part of the continuum Wightman function we compare to is

$$\Re\left[W_{M,\lambda}(X, X')\right] = -\frac{1}{2\pi}\ln|d(X, X')| + 0.53\,. \tag{3.48}$$

Figure 3.5 displays this function together with a scatter-plot of the discrete SJ amplitudes $\Re\left[w^{ij}\right]$ taken from region (i) in figure 3.4. Evidently, the fit is good, with a slight hint of a deviation at larger values of proper time which, if real, can be attributed to $\mathcal{O}(\delta/L)$ corrections, given that the centre region is still relatively large compared to L. From our previous analysis we know that $W_{M,\lambda}(X, X')$ approximates the continuum SJ state in the centre of the diamond, and so our data also supports the conclusion that the continuum and discrete SJ Wightman functions approximate each other.

The SJ vacuum in the corner and in the full diamond

For the corner, the type of plot we used for the centre is unsuitable because the continuum two-point functions we want to compare with depend on more variables than just the geodesic distance. Instead we plot the values of w directly against those of the continuum W with which we are comparing. More specifically, we use the coordinate values of the sprinkled points to calculate the values of a particular continuum function $W(X_i, X_j) =: W^{ij}$. We then plot a point on the graph whose vertical coordinate is W^{ij} and whose horizontal coordinate is w^{ij} at the corresponding pair of elements of the causet. In this manner, we will assess the correlation between the data sets w^{ij} and W^{ij} for 4 different continuum two-point functions: the exact continuum SJ function $W_{SJ,L}$ (before Taylor

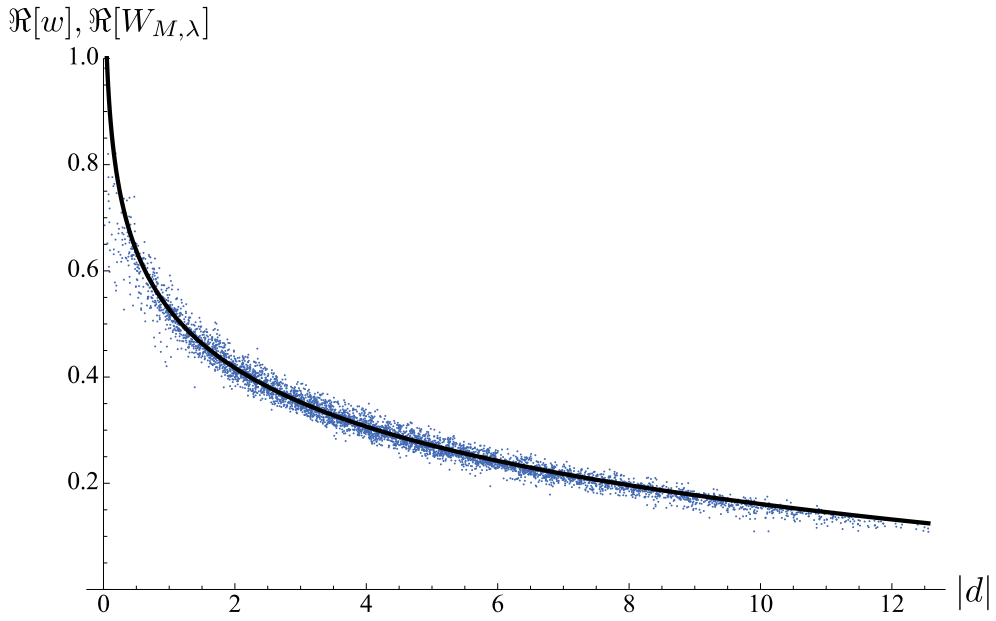

Figure 3.5: The real parts of the continuum two-point function $W_{M,\lambda}(X, X')$ (black line) with $\lambda = 0.02$ and the discrete SJ two-point function w_{ij} (blue scatter) in the centre of the finite diamond C_L with $L = 2^{\frac{9}{2}}$, plotted against the proper time $|d|$ for timelike separated events.

expansion), the Minkowski function $W_{M,\lambda}$ (3.23), the single mirror W_{mirror} (3.47), and the Rindler function $W_{R,\lambda}$ (3.27). Both the Rindler and Minkowski W-functions come with an arbitrary parameter λ, which shows up on the plots as an arbitrary vertical shift. We set this shift such that the intercept is zero.

The corner subregion (figure 3.4) contains 181 points, which produce a sample of 11230 pairs of timelike related points. The correlation plots for the real parts of the discrete and continuum propagators evaluated on this sample are shown in figure 3.6. Evidently, the plot of the exact SJ function exhibits a good fit with the causal set data, confirming again that the discrete and continuum formalisms agree. As expected, the correlation with the mirror two-point function is also high, implying that the ground state in the corner is indeed that of flat space in the presence of a mirror. (The slightly positive intercept in the causal set versus mirror plot, can plausibly be attributed to the ϵ correction and to $\mathcal{O}(\delta/L)$ effects, both of which would go away were the corner region made smaller.) As one would expect for the corner, the Minkowski and Rindler functions exhibit significantly worse correlations with the causet data-set.

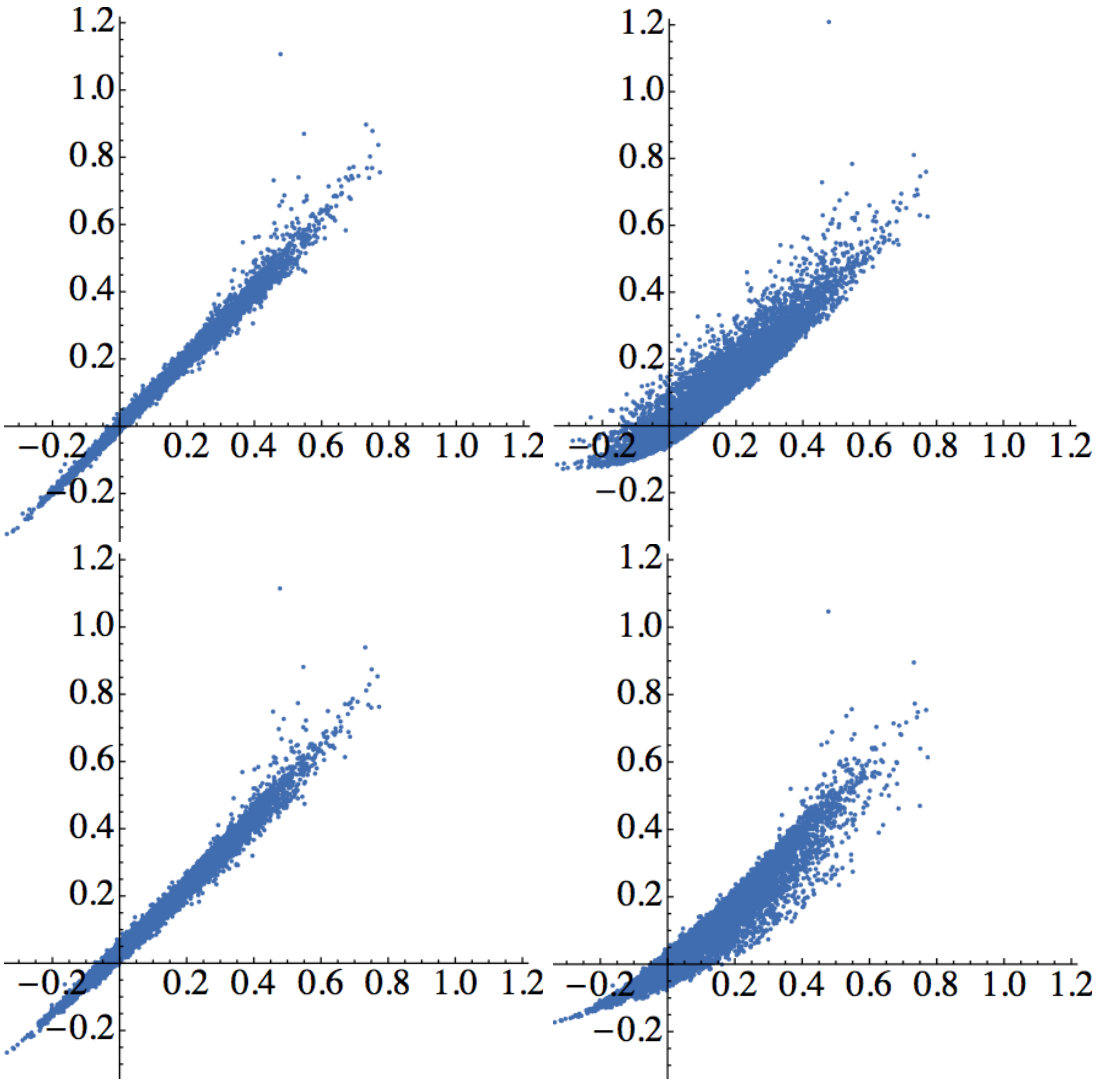

Figure 3.6: Correlation plots for the two-point functions in the corner of the causal diamond. The horizontal axis represents the causal set two-point function w^{ij}. The vertical axes represent, from top to bottom and left to right: the SJ, the Minkowski, the mirror, and the Rindler two-point functions.

Turning to the full diamond, we use a smaller overall causal set with $N = 256$, which yields a sample of 16393 pairs of timelike related points. To the four comparison functions above we add a fifth: the reflecting box (mirrors at both corners) $W_{\text{box},L}$. Of these five continuum two-point functions, one should expect that in addition to the SJ vacuum, only the reflecting box ground state would exhibit a reasonable degree of correlation with the causal set data. (As seen in equation (3.39) above, continuum SJ and reflecting-box are identical up to the error-term $\epsilon(u, v; u', v')$, which, however, can vary more appreciably now that we do not restrict ourselves to a small subregion of the diamond.) The correlation plots of figure 3.7 confirm this expectation, although the match with the discrete SJ function is not a sharp as in the case of the corner, perhaps reflecting the smaller overall sprinkling density.

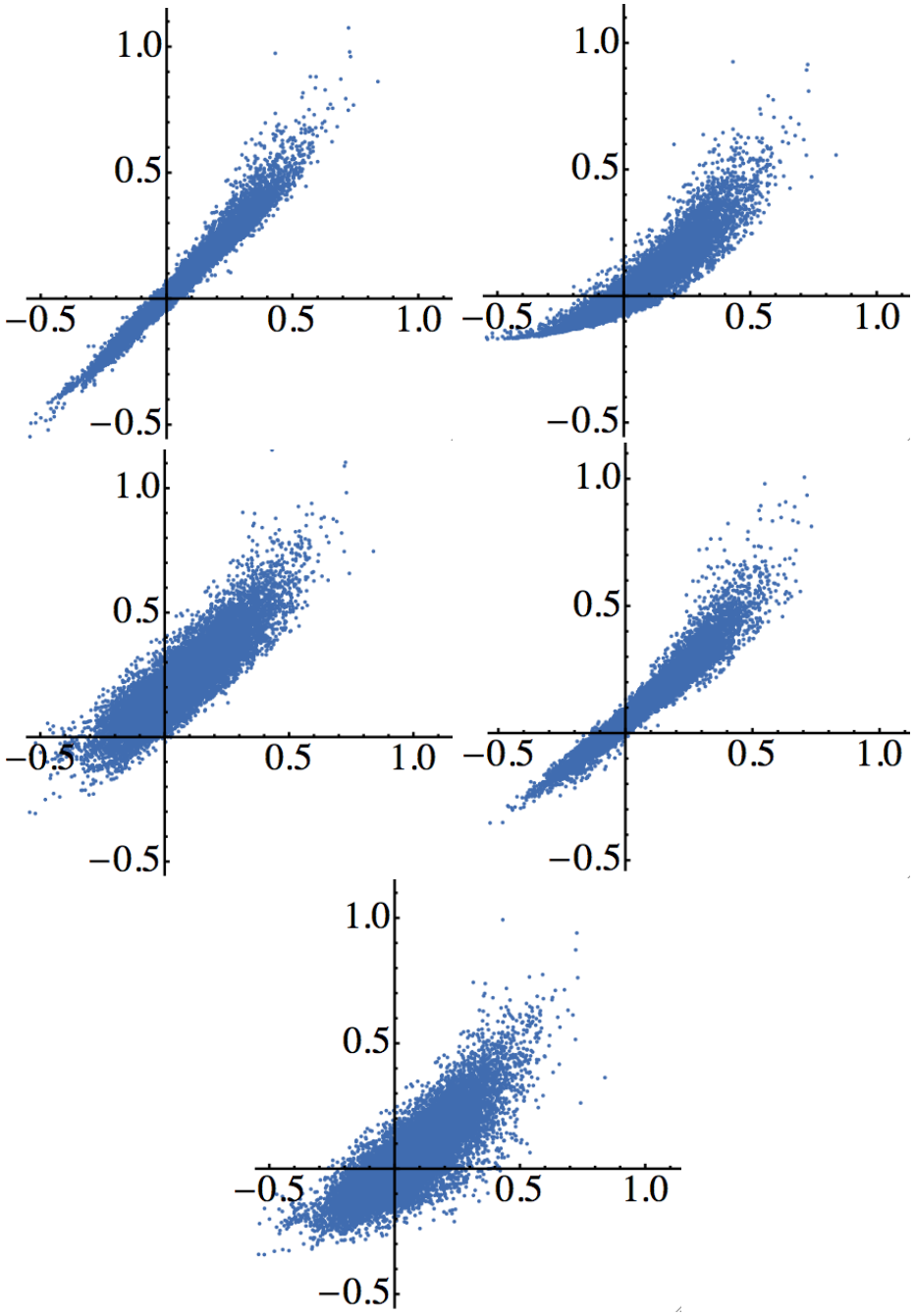

Figure 3.7: Correlation plots for the two-point functions in the full causal diamond. The horizontal axis represents the causal set two-point function w^{ij}. The vertical axes represent, from top to bottom and left to right: the SJ, the Minkowski, the left mirror, the box (two mirrors), and the Rindler two-point functions.

3.4 Causal Diamond, Massive Theory

To check whether the mirror result in the massless theory, for the Wightman function in the corner of the causal diamond, is an artifact of the massless theory, the analysis was repeated for the massive theory. The massive theory in the continuum was too complex to work with (due to the integrals involved), so calculations were instead carried out for the corresponding causal set theory.

The resulting scatterplots are shown in figure 3.8, for a 4096 element causal set. The mass was set to $m = 10$, the diameter of the diamond set to 1, and the corner region extended out to 0.2 along the diameter. The causal set two-point function was compared to the continuum expressions for three candidate Wightman functions: 1) The Wightman function for the massive theory in the Rindler vacuum, 2) the Wightman function for the massive theory in the mirror vacuum, and 3) the Wightman function for the massive theory in the Minkowski vacuum. These Wightman functions have the following expressions in the continuum [1, 36]:

$$W_{Mink}(x,t;x',t') = \frac{1}{2\pi}K_0[md] \tag{3.49}$$

$$\begin{aligned} &W_{Rind}(x,t;x',t') = \frac{1}{2\pi}K_0[md] \\ &- \frac{i}{2\pi}\int_{-\infty}^{\infty} \frac{K_0[m\sqrt{x^2-t^2+x'^2-t'^2+2\sqrt{(x^2-t^2)(x'^2-t'^2)}\cosh[s]}]}{(\pi^2+(s-|\operatorname{arctanh}[t/x]-\operatorname{arctanh}[t'/x']|)^2)}ds \end{aligned} \tag{3.50}$$

$$W_{Mirror}(x,t;x',t') = W_{Mink}(x,t;x',t') - W_{Mink}(x,t;-x',t') \tag{3.51}$$

where d as before is the geodesic distance $d = \sqrt{(t-t')^2-(x-x')^2}$.

This time, the scatterplots do not show enough contrast to make a good comparison possible. A rigorous statistical analysis would be necessary to assess the goodness of each fit, which we defer to future work. However, it does look like the Rindler function (at the top of figure 3.8) produces a slightly better fit than the others.

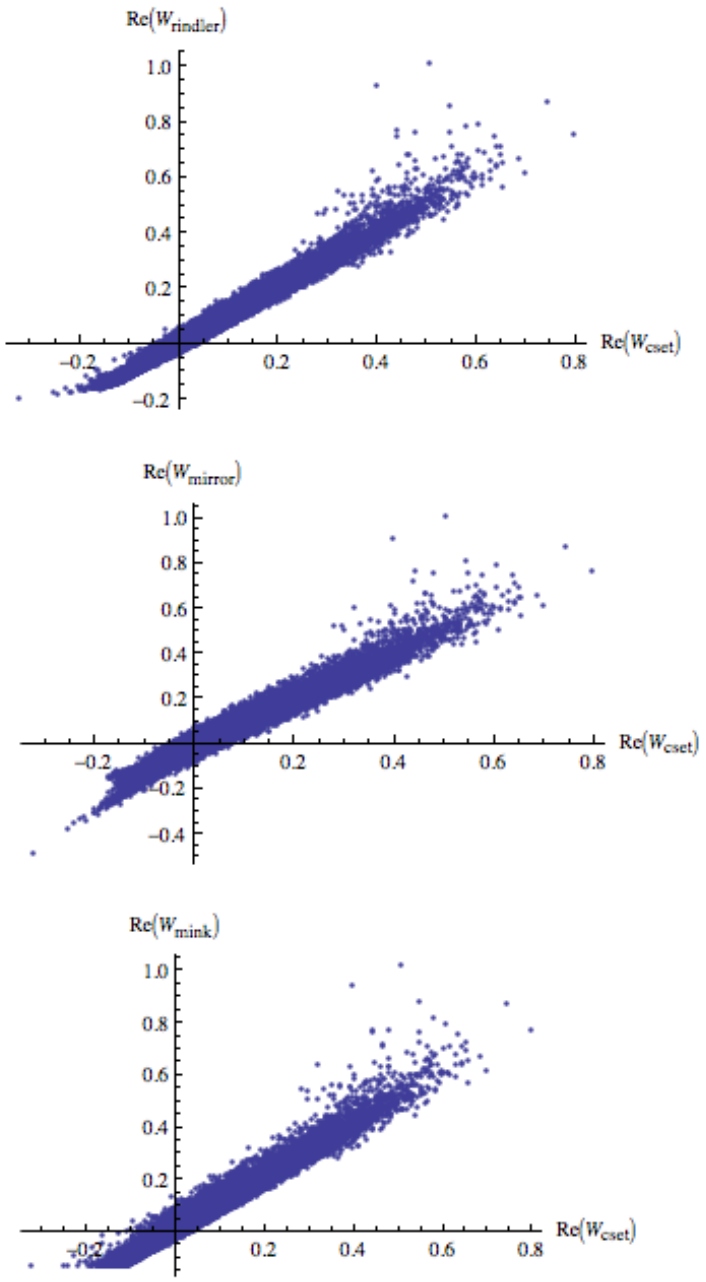

Figure 3.8: Correlation plots for the two-point functions in the corner of the causal diamond, for the massive theory ($m = 10$). The horizontal axis represents the causal set two-point function w^{ij}. The vertical axes represent, from top to bottom: the Rindler, the Mirror, and the Minkowski two-point functions.

3.5 Black Hole Vacua

In this section we will use a convention different from the one used in the previous sections, such that now $v \equiv t + x$ and $u \equiv t - x$. This is to be consistent with the references used [17, 32].

A major question we would like to address with the SJ proposal is: what sort of ground state is natural for a black hole spacetime? A few candidate vacuum states already exist for black hole spacetimes, but it is not clear which to work with. For example, for the eternal black hole there are three well-known vacua. If we call (u, v) lightcone coordinates of the Schwarzschild chart and (U, V) lightcone coordinates of the Kruskal chart, then we have: 1) The Boulware vacuum [8], which is defined with respect to positive frequency plane wave modes in Schwarzschild coordinates (u, v); 2) the Hartle-Hawking vacuum [22] defined by positive frequency plane wave modes in Kruskal coordinates (U,V), and 3) the Unruh vacuum [46] which is the *in* vacuum, defined with respect to positive frequency plane waves in (U, v).

A more physical picture which takes into account the formation of the black hole (rather than considering an eternal black hole), is the case of black hole formation through the collapse of a shell. This can be described by the Vaidya metric. We turn to this next.

3.6 Vaidya Spacetime

3.6.1 The metric

Vaidya spacetime has the following metric [17]:

$$ds^2 = -(1 - \frac{2M(v)}{r})dv^2 + 2dvdr + r^2 d\Omega^2 \tag{3.52}$$

It is a solution to Einstein's equation with a stress-energy tensor of the form

$$T_{vv} = \frac{dM(v)}{dv}\frac{1}{4\pi r^2} \tag{3.53}$$

It represents a purely ingoing radial flux of radiation described by $\frac{dM(v)}{dv}$, and can be used to model the collapse and formation of a black hole [32]. The simplest such model can be

obtained by considering a single collapsing null shell, located at for example $v = 0$, such that

$$M(v) = M\theta(v) \tag{3.54}$$

The resulting spacetime can then be separated into a Minkowski region for $v < 0$ and a Schwarzschild one for $v > 0$. It is convenient to define the null coordinates:

$$ds^2 = -du_m dv_m + r_m^2 d\Omega^2, \qquad v < 0 \tag{3.55}$$

$$ds^2 = -(1 - \frac{2M}{r_s})du_s dv_s + r_s^2 d\Omega^2, \qquad v > 0 \tag{3.56}$$

where $u_m = t_m - r_m$ and $v_m = t_m + r_m$ in (3.55), and $u_s = t_s - r_s^*$ and $v_s = t_s + r_s^*$ in (3.56). The m subscripts denote Minkowski coordinates and the s subscripts refer to Schwarzschild coordinates. The tortoise coordinate r^* is defined as usual:

$$r^* = r + 2M \ln(\frac{r - 2M}{2M}) \tag{3.57}$$

figure 3.9 shows the penrose diagram of the Vaidya spacetime, with the locations of the horizon and collapsing ray marked.

3.6.2 Solutions to the Wave Equation

Let us find solutions for a free massless scalar field, which we now call ψ, in this spacetime. As usual, ψ satisfies the Klein Gordon equation:

$$\Box\psi = 0 \tag{3.58}$$

Since the background spacetime is spherically symmetric, the solutions to this equation, can be expanded in terms of spherical harmonics $Y_{lm}(\theta, \phi)$:

$$\psi(x) = \sum_{l,m} \frac{\psi_l(t, r)}{r} Y_{lm}(\theta, \phi) \tag{3.59}$$

In the Minkowski region ($v < 0$) we have:

$$(-\frac{\partial^2}{\partial t^2} + \frac{\partial^2}{\partial r^2} - \frac{l(l+1)}{r^2})\psi_l = 0 \tag{3.60}$$

while in the Schwarzschild region we have:

$$(-\frac{\partial^2}{\partial t^2} + \frac{\partial^2}{\partial r^{*2}} - V_l)\psi_l = 0 \tag{3.61}$$

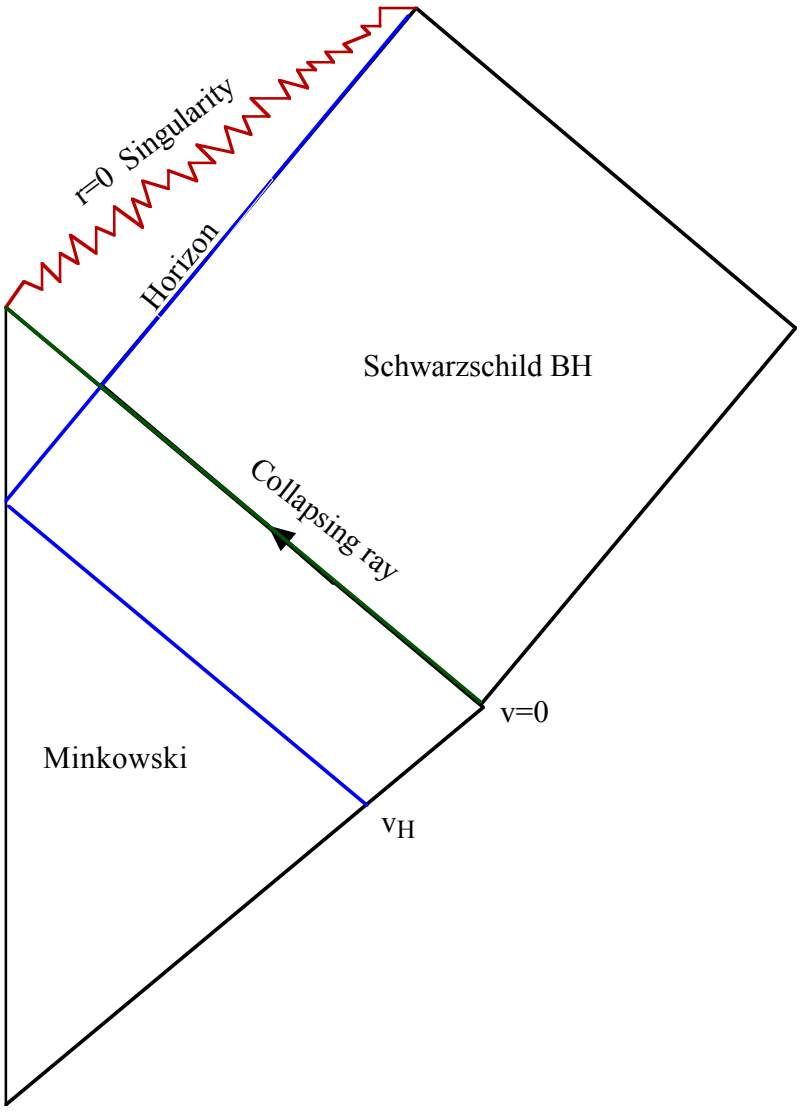

Figure 3.9: The Vaidya spacetime Penrose diagram.

where:

$$V_l = (1 - \frac{2M}{r})[\frac{l(l+1)}{r^2} + \frac{2M}{r^3}] \tag{3.62}$$

This potential vanishes at spatial infinity ($r, r^* = \infty$) and at the event horizon ($r = 2M, r^* = -\infty$), which suggests that the solutions to (3.61) behave asymptotically as $e^{\pm i\omega r*}$. In the following we will ignore the potential. A full treatment taking into account the scattering due to the potential would be extremely complex, and in any case, the important physics is believed to happen near the horizon, where the potential vanishes.

To apply the Sorkin-Johnston prescription, we need the Pauli-Jordan commutator function $i\Delta(x, x') = \langle 0|[\phi(x)\phi(x')]|0\rangle$. This Green function can be constructed using the Wightman function $W^+(x, x') = \langle 0|\phi(x)\phi(x')|0\rangle$, computed in any vacuum state of convenience, not necessarily the Sorkin-Johnston vacuum state that we wish to find.

We will now consider radial solutions to the field equations for our Vaidya model. These will help us to construct the Wightman function $W^+(x, x')$.

In the Minkowski region ($v < 0$)

$$(-\frac{\partial^2}{\partial t^2} + \frac{\partial^2}{\partial r^2})f = 0, \tag{3.63}$$

while in the Schwarzschild region

$$(-\frac{\partial^2}{\partial t^2} + \frac{\partial^2}{\partial r^{*2}})f = 0. \tag{3.64}$$

(we omit the spherical harmonics for now). Positive frequency ingoing mode solutions have the form of

$$f_\omega(v, r) = \frac{1}{\sqrt{4\pi\omega}}\frac{e^{-i\omega v}}{r} \tag{3.65}$$

and positive frequency outgoing mode solutions have the form of

$$f_\omega(u, r) = \frac{1}{\sqrt{4\pi\omega}}\frac{e^{-i\omega u}}{r} \tag{3.66}$$

with $\omega > 0$ in the Minkowski and exterior Schwarzschild regions, and $\omega < 0$ in the interior Schwarzschild region. We disregard the $\omega = 0$ mode. To describe modes that cross the

collapsing shell, we need an expression for $u_s(u_m)$. This relation can be obtained by requiring that the radius be continuous across the shell so that:

$$r(v=0,u_m) = \frac{-u_m}{2} = \frac{-u_s}{2} - 2M\ln[\frac{r(v=0,u_s)}{2M} - 1] = r(v=0,u_s) \tag{3.67}$$

leading to

$$u_s = u_m - 4M\ln[\frac{-4M-u_m}{4M}] \tag{3.68}$$

Thus, for example starting with a positive frequency outgoing mode in the exterior Schwarzschild region $\frac{1}{\sqrt{4\pi\omega}}\frac{e^{-i\omega u_s}}{r}$, we can trace it back in time to the Minkowski region where it will have the form $\frac{1}{\sqrt{4\pi\omega}}\frac{e^{-i\omega(v_m-4M\ln[\frac{-4M-v}{4M}])}}{r}\theta(v_H-v)$ on $\mathcal{J}^-$. Let us call these *up modes*. There are also modes which fall into the black hole. Positive frequency modes in the interior Schwarzschild region $\frac{1}{\sqrt{4\pi\omega}}\frac{e^{i\omega u_s}}{r}$, can be traced back to the Minkowski region where they will have the form $\frac{1}{\sqrt{4\pi\omega}}\frac{e^{i\omega(v_m-4M\ln[\frac{4M+v}{4M}])}}{r}\theta(v-v_H)$. Let us call these *dn modes*. We label as *in modes*, modes which always remain in Schwarzschild.

So we have three distinct sets of modes:

$$\psi^{in}_\alpha = \frac{1}{\sqrt{4\pi\omega}}\frac{e^{i\omega v}}{r}Y_{\ell m}(\theta,\phi) \tag{3.69}$$

$$\psi^{up}_\alpha = \frac{1}{\sqrt{4\pi\omega}}\frac{e^{-i\omega(v-4M\ln[\frac{-4M-v}{4M}])}}{r}Y_{\ell m}(\theta,\phi)\theta(-4M-v) \tag{3.70}$$

$$\psi^{dn}_\alpha = \frac{1}{\sqrt{4\pi\omega}}\frac{e^{i\omega(v-4M\ln[\frac{4M+v}{4M}])}}{r}\bar{Y}_{\ell m}(\theta,\phi)\theta(4M+v) \tag{3.71}$$

We have now included the spherical harmonics $Y_{\ell m}(\theta,\phi)$ in the solutions. The subscript α (and later on β) indicates all the quantum numbers (ℓ, m, ω).

We are now ready to expand our field in terms of these three mode solutions. A particularly convenient basis to work with is the so-called Wald's basis [32]. This basis forms a complete orthonormal basis, positive frequency with respect to the J^- Cauchy surface. It is defined using a linear combination of the modes we have introduced thus far.

Let:

$$\psi^d_\alpha = c_\alpha \psi^{dn}_\alpha + s_\alpha \bar{\psi}^{up}_\alpha \tag{3.72}$$

$$\psi^p_\alpha = c_\alpha \psi^{up}_\alpha + s_\alpha \bar{\psi}^{dn}_\alpha \tag{3.73}$$

where

$$c_\alpha = (1-\omega^2_\alpha)^{-1/2}, \tag{3.74}$$

$$s_\alpha = \omega_\alpha (1-\omega^2_\alpha)^{-1/2}, \tag{3.75}$$

and

$$\omega_\alpha = e^{-\frac{\pi\omega}{\kappa}}, \tag{3.76}$$

such that

$$c^2_\alpha - s^2_\alpha = 1. \tag{3.77}$$

Wald's basis is:

$$\Psi^{in}_\alpha = \begin{pmatrix} \psi^{in}_\alpha \\ \psi^d_\alpha \\ \psi^p_\alpha \end{pmatrix} \tag{3.78}$$

Using Wald's basis, the quantum field may be decomposed as

$$\psi_\alpha = \sum_\alpha [a_{in,\alpha}\psi^{in}_\alpha + a_{d,\alpha}\psi^d_\alpha + a_{p,\alpha}\psi^p_\alpha + h.c.] \tag{3.79}$$

Now, using the annihilation operators defined by this decomposition, $\mathbf{a}_{in,\alpha} = (a_{in,\alpha}, a_{d,\alpha}, a_{p,\alpha})$, and the corresponding vacuum state annihilated by them, $\mathbf{a}_{in,\alpha}|0,in\rangle$=0, we can construct a Wightman function:

$$W^+(x,x') = \langle in,0|\Psi(x)\Psi(x')|0,in\rangle = \sum_\alpha [\psi^{in}_\alpha(x)\bar{\psi}^{in}_\alpha(x') + \psi^d_\alpha(x)\bar{\psi}^d_\alpha(x') + \psi^p_\alpha(x)\bar{\psi}^p_\alpha(x')], \tag{3.80}$$

and the Pauli-Jordan function then is

$$\begin{aligned} i\Delta(x,x') &= W^+(x,x') - W^+(x',x) \\ &= \sum_\alpha [\psi^{in}_\alpha(x)\bar{\psi}^{in}_\alpha(x') + \psi^d_\alpha(x)\bar{\psi}^d_\alpha(x') + \psi^p_\alpha(x)\bar{\psi}^p_\alpha(x') \\ &- \psi^{in}_\alpha(x')\bar{\psi}^{in}_\alpha(x) - \psi^d_\alpha(x')\bar{\psi}^d_\alpha(x) - \psi^p_\alpha(x')\bar{\psi}^p_\alpha(x)], \\ &= \sum_\alpha [\psi^{in}_\alpha(x)\bar{\psi}^{in}_\alpha(x') - \psi^{in}_\alpha(x')\bar{\psi}^{in}_\alpha(x) + \psi^{dn}_\alpha(x)\bar{\psi}^{dn}_\alpha(x') - \psi^{dn}_\alpha(x')\bar{\psi}^{dn}_\alpha(x) \\ &+ \psi^{up}_\alpha(x)\bar{\psi}^{up}_\alpha(x') - \psi^{up}_\alpha(x')\bar{\psi}^{up}_\alpha(x)] \end{aligned} \tag{3.81}$$

We can now proceed with the SJ prescription. We want to treat $i\Delta(x,x')$ as an integral operator, under the L^2 norm, and find its positive eigenspace.

Alternatively, we can use the fact that the SJ Wightman function is uniquely determined by the following three conditions (as was discussed in the first part of this thesis):

1. *causality:* $i\Delta(X,X') = W(X,X') - W^*(X,X')$
2. *positivity:* $\int_{\mathcal{M}} dV \int_{\mathcal{M}} dV' f^*(X) W(X,X') f(X') \geq 0$
3. *orthogonal supports:* $\int_{\mathcal{M}} dV \int_{\mathcal{M}} dV' \int_{\mathcal{M}} dV'' f^*(X) W(X,X') W^*(X',X'') g(X'') = 0,$

$\forall$ functions $f, g : \mathcal{M} \to \mathbb{C}$, where $\int dV = \int d^d X \sqrt{-g(X)}$.

If we have a conjecture for what the SJ state might look like, checking the above conditions is a convenient way to find the SJ state. Here for our Vaidya model, a candidate state is the *in vacuum*, with its corresponding Wightman function (3.80). We can check the third condition above for this Wightman function. The first two conditions are satisfied by the two point function of any state, so it is the third condition that distinguishes our SJ ground state. To evaluate this, it is useful to define the following integrals:

$$\begin{aligned} F[\omega,k] &\equiv \int_{Dn} \psi_\alpha^{dn}(x') \psi_\beta^{dn}(x') \sqrt{|g|} dx' \\ &= (-1)^m \frac{\delta_{-\ell j}\delta_{-mn}}{4\pi\sqrt{k\omega}} (4M)^{i(\omega+k)4M} e^{-i(\omega+k)4M} (-i(k+\omega+i\epsilon))^{-1+i(\omega+k)4M} \\ &\quad \Gamma[1-i(\omega+k)4M)] \int_{Dn} dr' \end{aligned} \tag{3.82}$$

$$\begin{aligned} H[\omega,k] &\equiv \int_{Up} \psi_\alpha^{up}(x') \psi_\beta^{up}(x') \sqrt{|g|} dx' \\ &= (-1)^m \frac{\delta_{-\ell j}\delta_{-mn}}{4\pi\sqrt{k\omega}} (4M)^{-i(\omega+k)4M} e^{i(\omega+k)4M} (-i(k+\omega+i\epsilon))^{-1-i(\omega+k)4M} \\ &\quad \Gamma[1+i(\omega+k)4M)] \int_{Up} dr' \end{aligned} \tag{3.83}$$

$$
\begin{aligned}
J[\omega,k] &\equiv \int_{Dn\cap In}\psi^{dn}_{\alpha}(x')\psi^{in}_{\beta}(x')\sqrt{|g|}dx' \\
&= (-1)^m\frac{\delta_{-\ell j}\delta_{-mn}}{4\pi\sqrt{k\omega}}(4M)^{i\omega 4M}e^{-i(\omega-k)4M}(-i(\omega-k+i\epsilon))^{-1+i\omega 4M} \\
&\quad \Gamma[1-i\omega 4M)]\int_{Dn\cap In}dr' \qquad (3.84)
\end{aligned}
$$

$$
\begin{aligned}
M[\omega,k] &\equiv \int_{Up\cap In}\psi^{up}_{\alpha}(x')\psi^{in}_{\beta}(x')\sqrt{|g|}dx' \\
&= (-1)^m\frac{\delta_{-\ell j}\delta_{-mn}}{4\pi\sqrt{k\omega}}(4M)^{-i\omega 4M}e^{i(\omega+k)4M}(-i(k+\omega+i\epsilon))^{-1-i\omega 4M} \\
&\quad \Gamma[1+i\omega 4M)]\int_{Up\cap In}dr' \qquad (3.85)
\end{aligned}
$$

where α corresponds to the quantum numbers $\{\omega,\ell,m\}$ and β corresponds to $\{k,j,n\}$. Dn, Up, and In denote the region of applicability of the $\psi^{dn}(x)$ modes, $\psi^{up}(x)$ modes, and $\psi^{in}(x)$ modes respectively. The metric determinant is $g=-r^4\sin^2\theta$, and we used that the spherical harmonics obey the normalization condition:

$$
\int_0^{2\pi}d\phi\int_0^{\pi}d\theta\sin\theta\bar{Y}_{jn}(\theta,\phi)Y_{\ell m}(\theta,\phi)=\delta_{j\ell}\delta_{mn}, \qquad (3.86)
$$

and that

$$
Y_{\ell,m}(\theta,\phi)=(-1)^m\bar{Y}_{\ell,-m}(\theta,\phi). \qquad (3.87)
$$

We also used the relation

$$
\int_0^{\infty}x^a e^{-bx}=b^{-1-a}\Gamma(1+a). \qquad (3.88)
$$

To evaluate some of the integrals that are like (3.88), an additional regularization term ϵ was inserted (b$\rightarrow$ b+ϵ) to insure they converge [17]. This in effect plays the role of considering wave packets, where for example $\epsilon \ll 1$ would mean the wave packets are very narrow.

With the aid of the above expressions, it was found that the in-vacuum is not the SJ-vacuum state. Evaluating the SJ state directly, in terms of the positive eigenspace of $i\Delta$ is a difficult task, due to the integrals involved. Similar to the case of the massive theory for the causal diamond, it is more convenient to turn to the causal set to find the SJ state for our Vaidya model. A sprinkling of Vaidya spacetime would have to be simulated and the Green functions determined. We defer this to future work. Some work on causal set simulations of black holes has been done [23].

Chapter 4

Entropy

A large portion of this chapter will appear in [37].

4.1 A New Formula

In this section, we review a new formula for the entropy of a free scalar field in a globally hyperbolic region of spacetime. This will in large part be a summary of [43].

The new formula which we review uses the Wightman function of the field, $\langle 0|\phi(x)\phi(x')|0\rangle$, to define the entropy. In some cases, the derived entropy can also be interpreted as an entanglement entropy. An advantage of this approach is that it is applicable to both continuum spacetimes and to discrete causal sets. Entanglement entropy of black holes and intervals in flat spacetime, as we will see, often depend on a cutoff. In the context of causal sets there is a natural meaning for this cutoff, as it is the discreteness scale.

In conventional treatments, the entropy is defined with respect to a density matrix $\rho(\Sigma)$, where Σ is a hypersurface, as

$$S = Tr\rho \ln \rho^{-1} \tag{4.1}$$

If a Cauchy surface is divided into a subregion A and its complement B, then the reduced density matrix for region A is

$$\rho_A = Tr_B \rho \tag{4.2}$$

and the entanglement entropy corresponding to this reduced density matrix would be

$$S_A = -Tr\rho_A \ln \rho_A \tag{4.3}$$

The goal now is to express the entropy associated to a spacetime region in terms of the two-point function of the theory.

We start by considering a single degree of freedom, with a conjugate pair of variables q and p that satisfy $[q, p] = i$. These give us $\langle qq\rangle$, $\langle pp\rangle$, and $Re\langle qp\rangle$.

A Gaussian density matrix, in a basis of q, has the following expression

$$\rho(q, q') \equiv \langle q|\rho|q'\rangle \propto e^{(-\frac{A}{2}(q^2+q'^2)+\frac{iB}{2}(q^2-q'^2)-\frac{C}{2}(q-q')^2))}. \tag{4.4}$$

As already mentioned, the entropy will depend on ρ such that $S(\rho) = Tr\rho \ln \rho^{-1}$. Furthermore, S has to be dimensionless and invariant under unitary transformations. Given these conditions, S can only depend on the combination:

$$\langle qq\rangle\langle pp\rangle - (Re\langle qp\rangle)^2 = \frac{C}{2A} + \frac{1}{4} \tag{4.5}$$

In [6], it was shown that the entropy takes the form

$$S = -\frac{\mu \ln \mu + (1-\mu)\ln(1-\mu)}{1-\mu} \tag{4.6}$$

with

$$\mu = \frac{\sqrt{1+2C/A}-1}{\sqrt{1+2C/A}+1} \tag{4.7}$$

or

$$S = (\sigma + 1/2)\ln(\sigma + 1/2) - (\sigma - 1/2)\ln(\sigma - 1/2) \tag{4.8}$$

where $\pm i\sigma$ are the eigenvalues of $\Delta^{-1}R$ and where

$$i\Delta = 2Im \begin{pmatrix} \langle qq\rangle & \langle qp\rangle \\ \langle pq\rangle & \langle pp\rangle \end{pmatrix} \tag{4.9}$$

and

$$R = Re \begin{pmatrix} \langle qq \rangle & \langle qp \rangle \\ \langle pq \rangle & \langle pp \rangle \end{pmatrix} \tag{4.10}$$

(4.8) can be simplified further by using the eigenvalues of $\Delta^{-1}W = \Delta^{-1}R + i/2$ rather than those of $\Delta^{-1}R$ [1]. Calling these eigenvalues $\pm i\omega_{\pm}$ (where $\pm i\omega_{\pm} = i(1/2 \pm \sigma)$), the entropy can be written in the simpler form

$$S = \omega_+ \ln \omega_+ - \omega_- \ln \omega_- \tag{4.11}$$

To generalize (4.11), we simply extend it to a sum over the full spectrum of $\Delta^{-1}W$, or to work with real eigenvalues we can define the operator L by

$$\Delta^{-1}W = iL \tag{4.12}$$

and use its eigenvalues, which we call λ, to express the full entropy as the sum

$$S = \sum \lambda \ln |\lambda| \tag{4.13}$$

We can also define the eigenvalues λ as the solutions to the generalized eigenvalue problem

$$Wv = i\lambda \Delta v \tag{4.14}$$

and

$$\Delta v \neq 0. \tag{4.15}$$

The eigenvalues come in pairs of λ and $1 - \lambda$.

Hence we have arrived at a covariant formulation of the entropy that depends on Green functions of the theory.

If we take the Wightman function to be the SJ one from the previous chapter, W_{SJ}, the entropy vanishes. When we use W_{SJ}, the eigenvalues are either $\lambda = 1$, or $\lambda = 0$, and so the sum (4.13) vanishes. This is expected, since the SJ vacuum is a pure state.

As we have already mentioned, in some cases, the more generally defined entropy of a region (4.13) can be interpreted as an entanglement entropy. We will consider an example of such a case in the subsequent section. In Appendix B we compute the entropy of the harmonic oscillator.

[1] We work with the invertible part of Δ

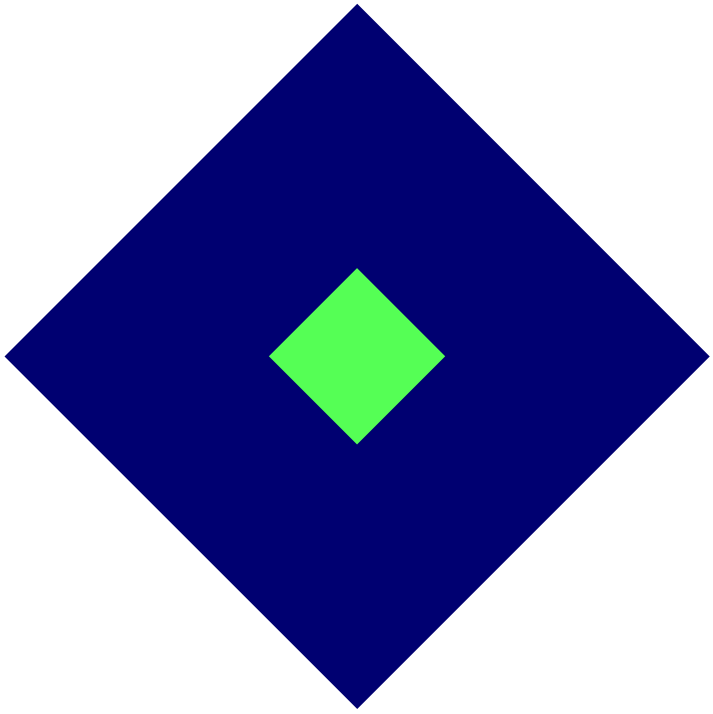

Figure 4.1: Spacetime of two causal diamonds.

4.2 Entanglement Entropy of Causal Diamonds

We now apply the formula in the previous section to compute the entanglement entropy in a spacetime with two causal diamonds, a smaller one and a larger one, as shown in figure 4.1, in 1+1. The results can be compared to results in CFT, where the entanglement between a shorter interval and a longer one is computed, the intervals being the Cauchy surfaces or diameters of the diamonds here. Usually periodic boundary conditions are imposed in the CFT calculations. For the massless theory, the entropy has been found to take the form [9, 10] (see also [35])

$$S = \frac{1}{3} \ln[\frac{L}{\pi a} \sin(\frac{\pi \ell}{L})] + c_1, \tag{4.16}$$

where a is the UV cutoff of the theory, ℓ is the length of the shorter interval, L is the length of the longer interval, and c_1 is a non-universal constant. In the limit that the

smaller interval is much smaller than the larger one ($\lim \frac{\ell}{L} \to 0$), the entropy reduces to

$$S = \frac{1}{3} \ln[\frac{\ell}{a}] + c_1. \tag{4.17}$$

Hence it only depends on the length of the smaller interval and the UV cutoff of the theory. The dependence on the length of the larger interval drops out. For the massive theory, the entropy has been found to take the form [9, 10]

$$S = -\frac{1}{6} \ln[ma] + c_1. \tag{4.18}$$

We now discuss a summary of our calculation for the massless theory in the continuum, with a UV cutoff a, using the new proposal. We need the Green functions $i\Delta$ and W for our model. In Minkowski lightcone coordinates $u = \frac{t+x}{\sqrt{2}}$ and $v = \frac{t-x}{\sqrt{2}}$, the Pauli-Jordan function has the form of (3.28):

$$i\Delta(u, v; u', v') = -\frac{i}{2}[\theta(u - u') + \theta(v - v') - 1] \ . \tag{4.19}$$

and for W, we will use the asymptotic form of W_{SJ} for a large causal diamond when spacetime points of interest lie far from the corners of the diamond. We found this had the form of (3.43):

$$W_{\text{centre}}(u, v; u', v') = -\frac{1}{4\pi}\ln|\Delta u \Delta v| - \frac{i}{4}\text{sgn}(\Delta u + \Delta v)\theta(\Delta u \Delta v) - \frac{1}{2\pi}\ln\frac{\pi}{4\tilde{L}} + \epsilon_{\text{centre}} + \mathcal{O}\left(\frac{\delta}{\tilde{L}}\right), \tag{4.20}$$

where $\epsilon_{\text{centre}} \approx -0.063$ and δ collectively denotes the coordinate differences $u - u', v - v', u - v', v - u'$. It will be more convenient to work with $\tilde{\ell}$ and $\tilde{L}$, the half side lengths of the smaller and larger diamonds respectively, rather than the diameters ℓ and L, although we express our final answer in terms of the latter ($\ell = 2\sqrt{2}\tilde{\ell}$ and $L = 2\sqrt{2}\tilde{L}$). We will scale $\tilde{\ell} \equiv 1$ and $\tilde{L} \equiv 100$, such that the ratio of the diameter of the smaller diamond to the larger one is 0.01 and we are in a regime where (4.17) applies.

We saw that expressed differently, (4.20) is just the Minkowski Wightman function with a particular value of the infrared cutoff $\lambda_{IR} = \frac{\pi}{4\sqrt{2}} e^{-\gamma - 2\pi\epsilon_{\text{centre}}} \tilde{L}^{-1} \approx 0.46 \times \tilde{L}^{-1}$:

$$W_M(u, v; u', v') = -\frac{1}{4\pi} \lim_{\epsilon \to 0^+} (-\frac{1}{4\pi} \ln\left[-\mu^2(\Delta u - i\epsilon)(\Delta v - i\epsilon)\right]) + \mathcal{O}(\lambda_{IR}\Delta), \tag{4.21}$$

where $\mu = \lambda_{IR} e^{\gamma}$, γ is the Euler-Mascheroni constant, and $\Delta u = u - u'$, $\Delta v = v - v'$, and the Δ in the final term stands collectively for Δu and Δv. We will use

$$W(u, v; u', v') = \frac{1}{4\pi} \lim_{\epsilon \to 0^+} (-\frac{1}{4\pi} \ln \left[-\mu^2 (\Delta u - i\epsilon)(\Delta v - i\epsilon) \right]) \tag{4.22}$$

with $\mu = 0.00825061$ (since we have set $\tilde{L} \equiv 100$).

We want to solve

$$W v = i\lambda \Delta v \tag{4.23}$$

and

$$\Delta v \neq 0. \tag{4.24}$$

We use the basis that diagonalizes $i\Delta$, which consisted of two sets of eigenfunctions:

$$f_k(u, v) := e^{-iku} - e^{-ikv}, \qquad \text{with } k = \frac{n\pi}{\tilde{\ell}},\ n = \pm 1, \pm 2, \ldots \tag{4.25}$$

$$g_k(u, v) := e^{-iku} + e^{-ikv} - 2\cos(k\tilde{\ell}), \qquad \text{with } k \in \mathcal{K}, \tag{4.26}$$

where $\mathcal{K} = \left\{ k \in \mathbb{R} \,|\, \tan(k\tilde{\ell}) = 2k\tilde{\ell} \text{ and } k \neq 0 \right\}$. The eigenvalues were $\tilde{\lambda}_k = \tilde{\ell}/k$ ($\tilde{\lambda}$ is used to avoid confusion with λ in (4.23)). The L^2-norms are $||f_k||^2 = 8\tilde{\ell}^2$ and $||g_k||^2 = 8\tilde{\ell}^2 - 16\tilde{\ell}^2 \cos^2(k\tilde{\ell})$.

The UV cutoff will correspond to the k at which we truncate our basis. $i\Delta$ is diagonalized by this basis, so its representation is trivial. For W, we must compute $\langle f_k | W | f_{k'} \rangle$ and $\langle g_k | W | g_{k'} \rangle$. The terms $\langle f_k | W | g_{k'} \rangle$ vanish, so W is block diagonal in this basis. We compute these two inner products and treat each block separately in (4.23). Summing over the resulting eigenvalues, we obtain the entropy associated to each block. Figures 4.2 and 4.3 illustrate the results. Figure 4.4 shows the total entropy, as a function of the UV cutoff $1/a$.

Our fit matches

$$S = \frac{1}{3} \ln \left[\frac{\ell}{a} \right] + c_1 \tag{4.27}$$

with $c_1 \approx 0.3612$. Hence we have arrived at the expected CFT result.

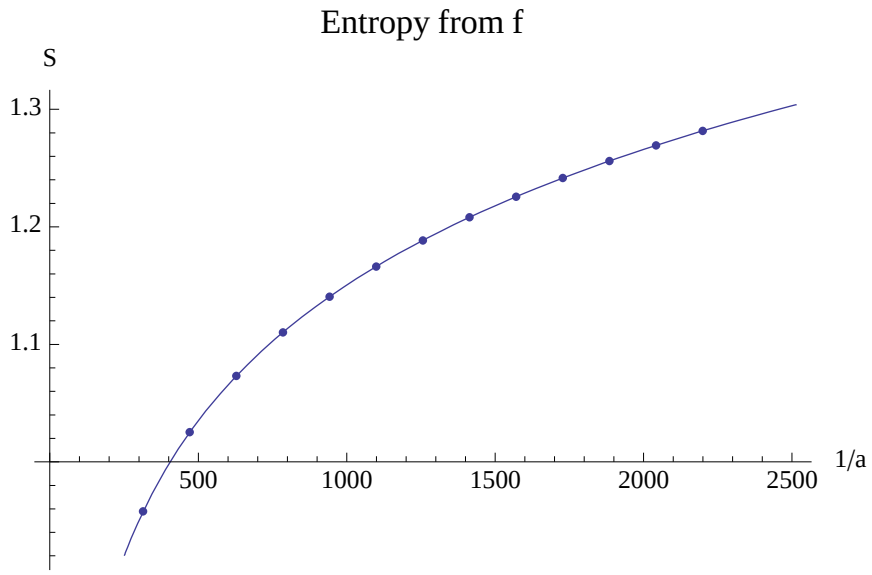

Figure 4.2: Entropy S versus the UV cutoff $1/a$, for the f block.

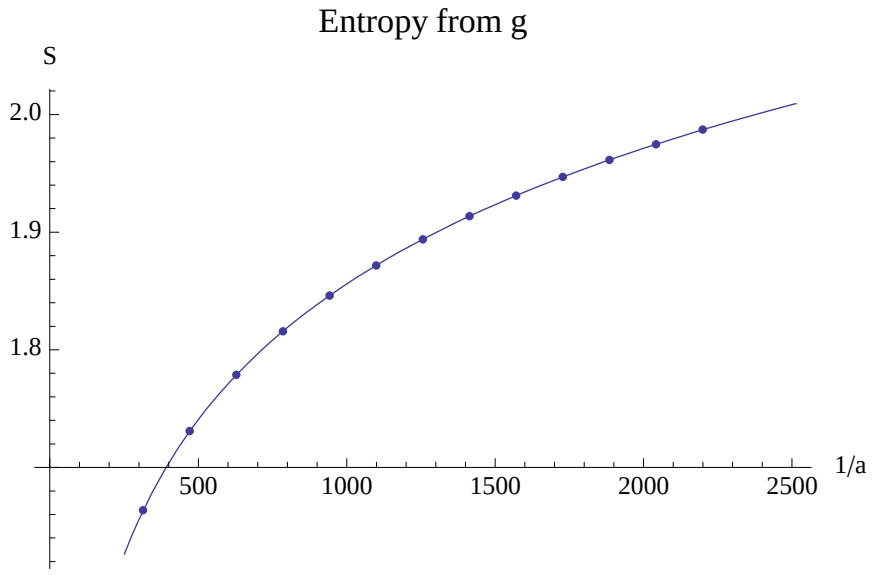

Figure 4.3: Entropy S versus the UV cutoff $1/a$, for the g block.

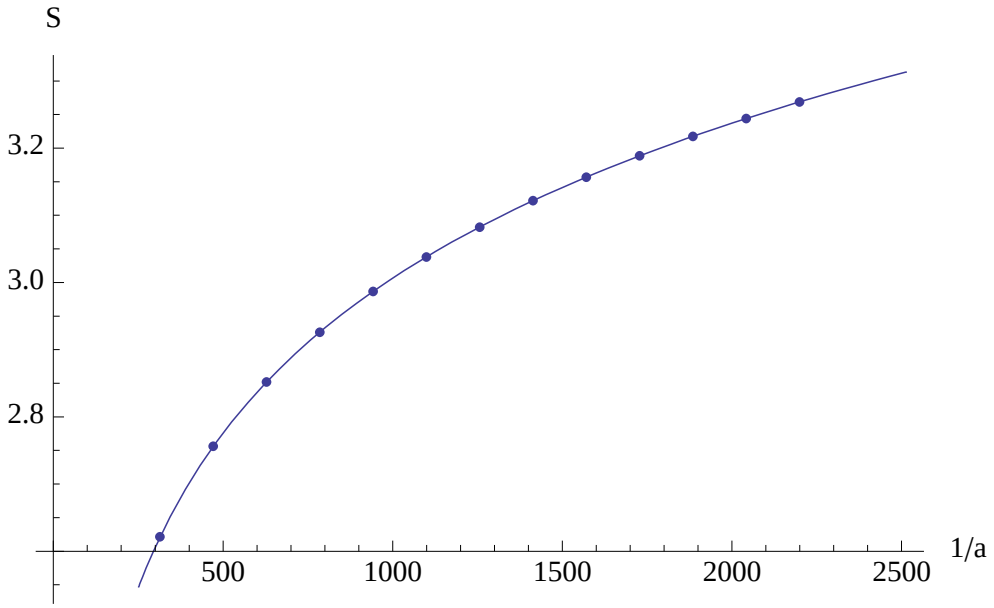

Figure 4.4: The full entropy S versus the UV cutoff $1/a$.

4.3 Causal Set Results

We also carried out calculations for causal set simulations of the same model of causal diamonds, shown in figure 4.5. We find that the entropies are large compared to the CFT predictions. For example, for $m = 0$, $\rho = 1$, $L = 90$, $\ell = 18$, the entropy obtained was $S \approx 75$, while in comparison the CFT prediction is $S^{CFT} \approx 1$.

A surprising result was obtained by keeping the ratio ℓ/L fixed, while increasing the number of sprinkled points. This was done for fixed ratios of $\ell/L = 0.2$ and $\ell/L = 0.4$. It was found that the entropy increases linearly with the number of sprinkled points. Figures 4.6 and 4.7 show this linear relation. The results fit $S = aN + b$ with $\{a = 0.513004, b = -4.12018\}$ and $\{a = 0.381562, b = -7.31323\}$ for $\ell/L = 0.2$ and $\ell/L = 0.4$ respectively.

Another analysis was carried out to determine the effect of coarse-graining. Here we no longer considered two regions and had only one causal diamond. We chose to coarse-grain by 90%, each time removing points with a probability 0.1. Here also, a simple relation was obtained. The entropy depended parabolically on the number of points remaining after coarse-graining. Initially, when all points are present, the entropy is 0. It rises until about half the points remain, after which it drops, symmetrically, until it reaches near 0 again around when there are no more points left. The results fit $S = aN^2 + bN + c$ with $\{a = -0.000140482, b = 0.563276, c = 41.064\}$. The relation is shown in figure 4.8, where the entropy is plotted versus the number of points in the causal diamond. Initially the diamond contained 4048 sprinkled points.

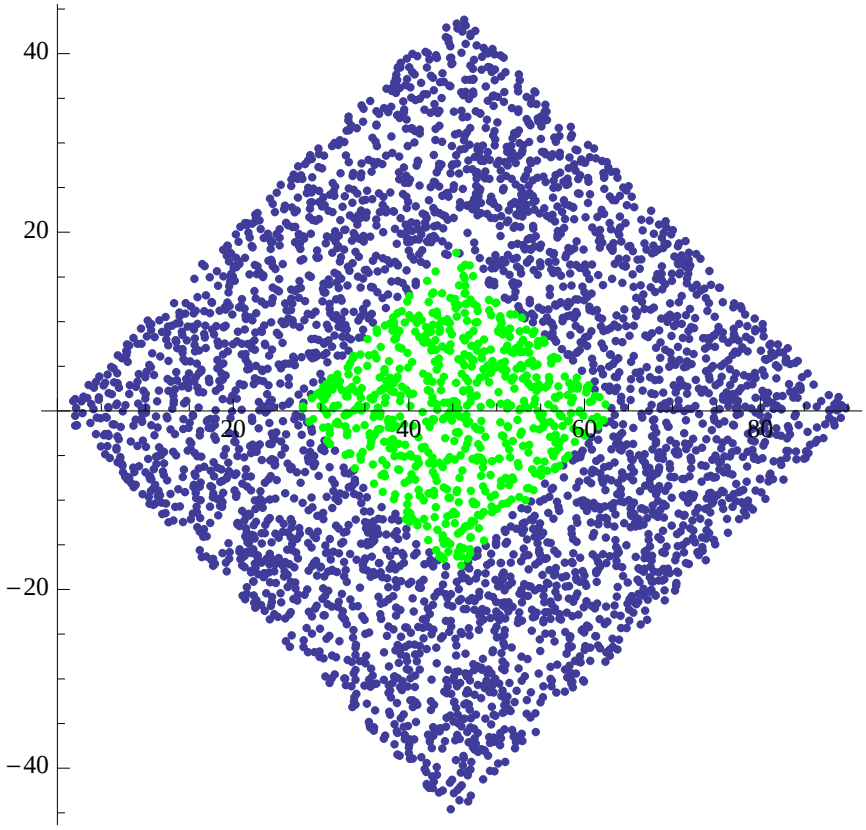

Figure 4.5: Causal Sets of two causal diamonds.

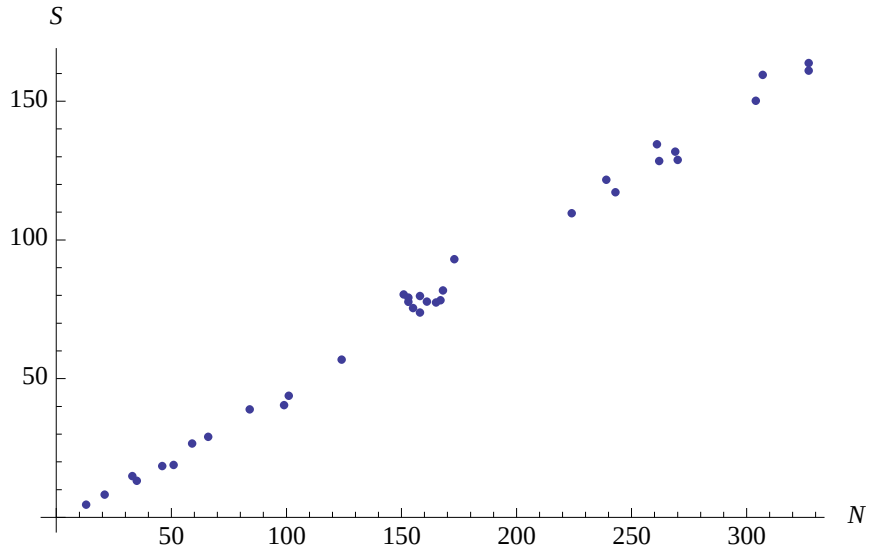

Figure 4.6: S vs N when $\ell/L = 0.2$. N is the number of causet elements in the smaller diamond.

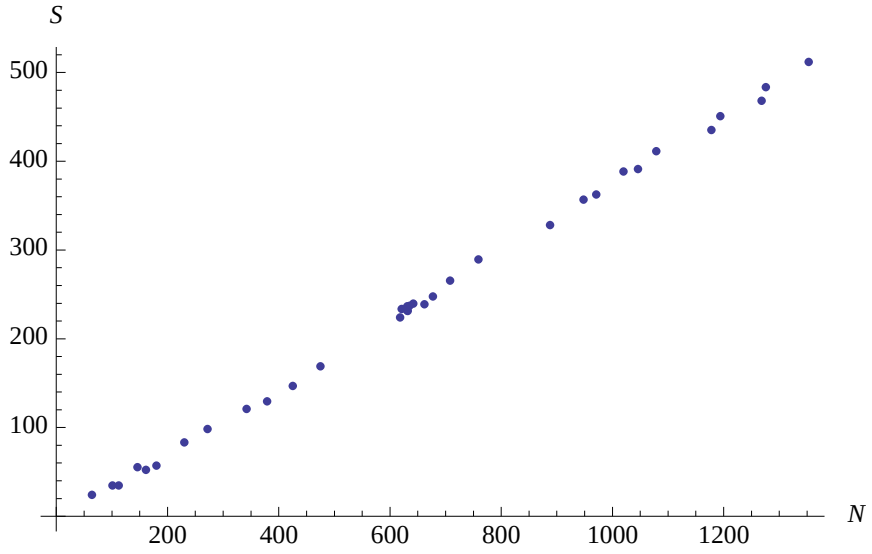

Figure 4.7: S vs N when $\ell/L = 0.4$. N is the number of causet elements in the smaller diamond.

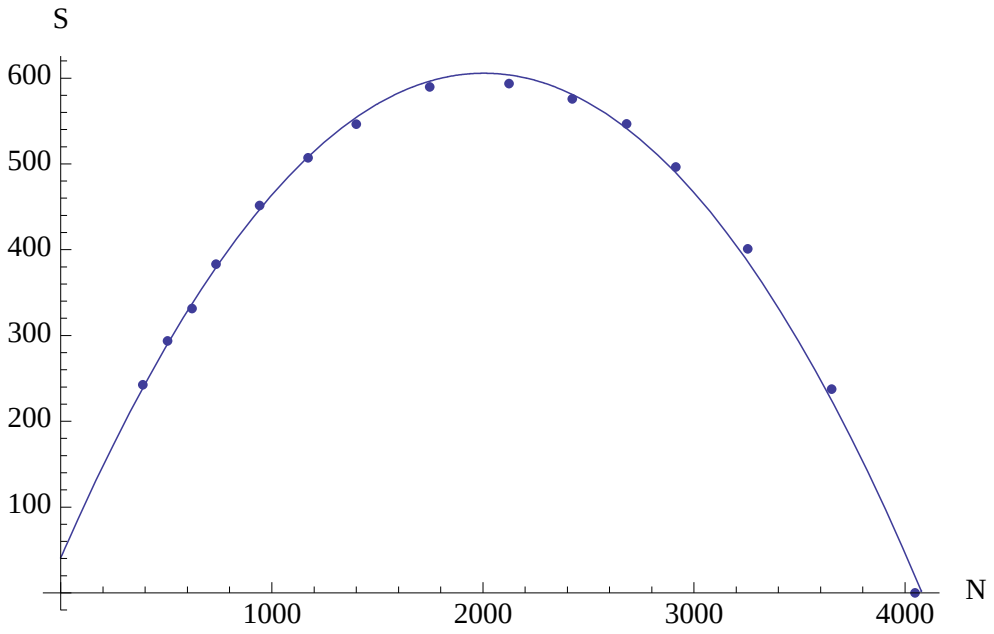

Figure 4.8: S vs. N under coarse-graining by 0.9

Chapter 5

Concluding remarks

At the end of his classic textbook 'Aspects of Quantum Field Theory in Curved Space-Time,' [20] S.A. Fulling points out the central tension in the subject as traditionally studied:

> One of the striking things about the subject is the intertwining of the conceptual issues with the mathematical tools. Historically there has been a close association between relativity and differential geometry, while rigorous research in quantum theory has looked more toward functional analysis. Field quantisation in a gravitational background brings these two alliances into head-to-head confrontation: A field is a function of a time and a space variable,
>
> $$\phi(t, \mathbf{x}).$$
>
> Relativity and modern geometry persuade one with an almost religious intensity that these variables must be merged and submerged; the true domain of the field is a space-time manifold:
>
> $$\phi(\underline{x}), \quad \underline{x} \to \{x^\mu\}$$
>
> But quantum theory and its ally, analysis, are constantly pushing in the opposite direction. They want to think of the field as an element of some function space, depending on time as a parameter:
>
> $$\phi_t(\mathbf{x}).$$

The split of spacetime into space plus time that Fulling assumes to be inherent in the quantum aspect of the field theory is actually an artifact of the choice to conceive of a quantum field as if it were the canonical quantisation of a classical Hamiltonian system. In a canonical approach, defining the Hamiltonian tends to demand the foliation of spacetime into spacelike hypersurfaces. However, there is an alternative, long ago identified by Dirac as more fundamental because it is essentially relativistic: the quantum analogue of the classical Lagrangian approach, namely the path integral [15].

Like the path integral, the SJ vacuum is also relativistic in character, depending, as it does, on the geometry of the whole spacetime region via the causal structure encoded in the retarded Green function. Its construction is inherently covariant, and at no point is there a need to introduce mode-functions defined on a hypersurface, except as dictated by calculational convenience. The formulation of the quantum theory along these lines bears no resemblance to the "canonical quantisation" process: one does not solve the classical equations of motion or identify canonically conjugate variables or promote them to operators satisfying canonical commutation relations. Such a formulation seems much more compatible with a path integral approach to quantum theory, and indeed the SJ proposal serves as the starting point for the construction of a histories-based formulation of quantum field theory on a causal set [42] which admits a natural generalization to interacting scalar fields and takes us one step further towards a quantum theory of causal sets.

In this work, we have determined the SJ vacuum of a massless scalar field in the two-dimensional "causal diamond" spacetime and compared it with suitable reference states in the full Minkowski spacetime and in the Rindler wedge. Both of these reference "states", the "Minkowski vacuum" and the "Fulling-Rindler vacuum", suffer from infrared pathologies, but to the extent that they are meaningful we can compare them with the SJ state in the limit that the size of the diamond goes to infinity.

When we look near the centre of the diamond, we find that the SJ Wightman function agrees with the "Minkowski vacuum", just as one might have expected. However, when we look in the corner of the diamond we do not see something having the form of a "Fulling-Rindler vacuum". Instead we recognise the flat-space vacuum in the presence of a static mirror at that corner. This is confirmed by the numerical results. Thus, the continuum calculations in section 3.1 giving the SJ state in the Rindler wedge do not agree with the limiting procedure of constructing the SJ state in the finite diamond and letting the size of the diamond tend to infinity, whilst keeping the arguments of the two-point function at fixed locations with respect to the corner. Such a ground state, if it is defined at all, should be unique and be independent of any (physically sensible) limiting procedure. Of

course, one cannot really speak of a disagreement between two functions, one of which is ill-defined, but the fact remains that our limiting procedure yields very different results for the centre versus the corner of the diamond. It seems likely that these disagreements and ambiguities stem from the infrared divergences of the two-dimensional massless theory, and if one were to work instead with a massive field,[1] the SJ state for the wedge would be unique and in agreement with both the Fulling-Rindler vacuum and the limit of the diamond's SJ state. Some of these questions will be investigated in future work, but preliminary numerical results for the massive scalar field in the sprinkled diamond indicate that the discrete SJ function does fit the Fulling-Rindler vacuum better than the state with a mirror present.

In this work we also considered a recent formula for the entropy associated to a spacetime region, for a free scalar field. There has been a significant amount of interest in formulating measures of quantum entanglement. Entanglement entropy is of course a powerful such measure that can be readily applied to systems of interest such as quantum spin chains. The formula that we use, much like the SJ proposal, is faithful to using the geometry of the entire spacetime in a covariant manner. There is no need to split spacetime into space plus time and to construct hypersurfaces with which to compute the entropy.

We determined the entanglement entropy for a free massless scalar field in a causal diamond in 1+1 Minkowski spacetime, when the subregion is a smaller causal diamond. In the continuum we obtained the results found in CFT for the same model. The entropy scales logarithmically with the ratio of the diameter of the smaller diamond to the UV cutoff, with a coefficient of 1/3. In the causal set, there are additional subtleties which remain to be understood.

The SJ proposal and the entropy formula that we have considered take the relativistic view and define the ground state and entropy of a free quantum scalar field theory using Green functions of the theory. They are applicable in globally hyperbolic spacetimes, where unique retarded and advanced Green functions of the theory exist. Due to their spacetime nature, they can be applied to continuum or discrete spacetimes. In particular, they apply in causal sets, and thus they play an important role in setting up a quantum theory of causal sets.

[1] One might also consider working with the gradient of the field, which would be less sensitive to IR peculiarities. However, this in itself would not erase the difference between (3.27) and (3.46), if the two point function of the gradient is the same as the gradient of the two point function.

APPENDICES

Appendix A

Corrections to the SJ two-point function

In evaluating the second sum (3.36) of the continuum SJ two-point function (3.33), we made the approximation $\mathcal{K} \to \mathcal{K}_0$. For a given pair of spacetime points, this will induce an error in the two-point function, which (see (3.37) and (3.33)) is given by

$$\epsilon(u,v;u',v') = \sum_{n=1}^{\infty} \left[\frac{L}{k_n} \frac{1}{||g_{k_n}||^2} g_{k_n}(u,v) g^*_{k_n}(u',v') - \frac{L}{k_{0,n}} \frac{1}{||g_{k_{0,n}}||^2} g_{k_{0,n}}(u,v) g^*_{k_{0,n}}(u',v') \right], \tag{A.1}$$

where k_n and $k_{0,n}$ denote the n^{th} terms in $\mathcal{K}$ and $\mathcal{K}_0$, respectively. The contributions to the right hand side come mostly from long wavelength (small n) terms, since the approximation $\mathcal{K} \to \mathcal{K}_0$ becomes increasingly accurate for large n (see figure 3.3). This means that we should expect ϵ to be constant over small subregions of the diamond. We will first test this expectation numerically, restricting ourselves for simplicity to timelike related pairs of points

To estimate the mean and the variation of $\epsilon(u,v;u',v')$ over different pairs of spacetime points in a subregion associated with the centre (i) or corner (ii) of the diamond, we evaluated $\epsilon(u,v;u',v')$ on a random sample P of pairs of timelike related points within that region. We evaluated (A.1) by truncating the sums on the right hand side at a stage large enough for the sum to have converged sufficiently. We then calculated the mean value of $\epsilon(u,v;u',v')$ and its standard deviation on the sample P. We present the results for the real part of $\epsilon(u,v;u',v')$ below, since we are mainly interested in the real part of the Wightman function W. (The imaginary part of W is proportional to Δ and therefore

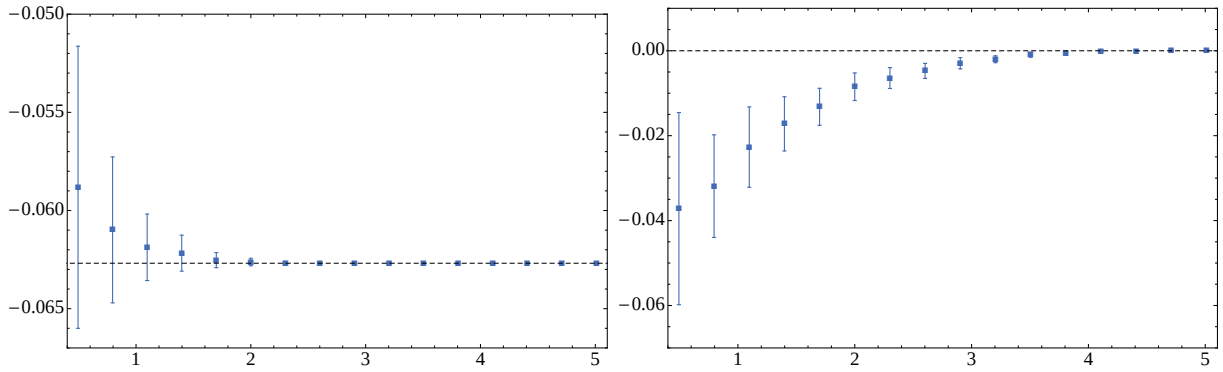

Figure A.1: The mean and standard deviation of $\epsilon(u, v; u', v')$ in the centre (left) and in the corner (right). The vertical axis corresponds to $\epsilon(u, v; u', v')$ and the horizontal axis is $-\log_{10}(V_{\text{sub}}/V)$.

known exactly. Moreover, the imaginary part of $\epsilon(u, v; u', v')$ was consistent with zero in all the regions we investigated numerically.)

Look at subregions in the centre and corner of the form depicted in figure 3.4: a square in the centre, a triangle in the corner. Fix the linear dimension of the subregion $D \ll L$ and denote its spacetime volume by V_{sub}. Increase the size L of the full diamond while keeping D fixed, thereby decreasing the volume ratio V_{sub}/V. The mean and standard deviation of $\epsilon(u, v; u', v')$ obtained in this way are shown in figure A.1 for different values of V_{sub}/V ranging from $\mathcal{O}(10^{-1})$ to $\mathcal{O}(10^{-6})$. These results were obtained by truncating the sum (A.1) at $n = 50$, which provides sufficient accuracy. We observe that the standard deviation in $\epsilon(u, v; u', v')$ indeed quickly becomes negligible as V_{sub}/V is decreased. The mean of $\epsilon(u, v; u', v')$ tends to a constant value in the centre given by $\epsilon_{\text{centre}} = -0.0627$ and it vanishes in the corner: $\epsilon_{\text{corner}} = 0$. Notice that these results are unchanged under a simultaneous rescaling of L and D: the mean and standard deviation of $\epsilon(u, v; u', v')$ depend only on the ratio V_{sub}/V.

It is worth noting that the asymptotic values for the mean of ϵ seen at large L above agree with the values of $\epsilon(u, v; u', v')$ that we obtain if we simply evaluate the infinite sum on a pair of coincident points in the centre of the diamond, $(u, v) = (u', v') = (0, 0)$, or in

the corner $(u, v) = (u', v') = (-L, L)$. In the centre, the sum (A.1) reduces to

$$\epsilon(0,0;0,0) = \sum_{n=1}^{\infty} \left[\frac{\left(1 - \sqrt{4x_n^2 + 1}\right)^2}{2x_n \left(4x_n^2 - 1\right)} - \frac{1}{\pi(2n-1)} \right], \tag{A.2}$$

where x_n is the n^{th} positive solution to $\tan(x) = 2x$. This sum can be evaluated to arbitrary precision using numerical solutions for x_n, and it tends to $\epsilon(0,0;0,0) = -0.0627$, corresponding to the horizontal asymptote in the centre plot of figure A.1. In the corner, both terms in (A.1) vanish because the g_k modes (3.31) are identically zero at $(-L, L)$ for all $k_n \in \mathcal{K}$ and $k_{0,n} \in \mathcal{K}_0$. It follows that $\epsilon(-L, L; -L, L) = 0$, corresponding to the horizontal asymptote in the corner plot of figure A.1.

Appendix B

Entropy of the Harmonic Oscillator

Let us now apply the formalism presented in Chapter 4 to the harmonic oscillator in one dimension.

First we compute the entropy of the harmonic oscillator using the standard thermodynamic relation

$$S = \frac{\partial}{\partial T}(T \ln Z) \tag{B.1}$$

For the harmonic oscillator, with energies $E_n = (n + \frac{1}{2})\hbar\omega$, the partition function Z takes the form

$$Z = \frac{e^{-\frac{\beta\omega}{2}}}{1 - e^{-\beta\hbar\omega}} \tag{B.2}$$

where β is the inverse temperature. Using (B.2) and (B.1), the entropy we obtain is

$$S = -\ln[1 - e^{-\beta\hbar\omega}] + \frac{e^{-\frac{\beta\omega}{2}}}{1 - e^{-\beta\hbar\omega}} \tag{B.3}$$

Now let us compute the entropy of the harmonic oscillator using the prescription of Chapter 4.

Our Pauli-Jordan function is

$$i\Delta(t, t') = \frac{1}{2\omega}(e^{-i\omega(t-t')} - e^{i\omega(t-t')}) \tag{B.4}$$

and our Wightman function takes the form

$$W(t,t') = \frac{1}{2\omega}(\frac{e^{-i\omega(t-t')} + e^{i\omega(t-t')}}{e^{\beta\omega} - 1} + e^{-i\omega(t-t')}) \tag{B.5}$$

Simultaneous eigenfunctions of these two Green functions, treated as operators, turn out to be positive and negative frequency plane waves $e^{-i\omega t}$ and $e^{i\omega t}$

$$\int i\Delta(t,t')e^{-i\omega t'}dt' = \frac{1}{2\omega}2\pi\delta(0) \tag{B.6}$$

$$\int i\Delta(t,t')e^{i\omega t'}dt' = -\frac{1}{2\omega}2\pi\delta(0) \tag{B.7}$$

$$\int W(t,t')e^{-i\omega t'}dt' = \frac{e^{\beta\omega}}{2\omega(e^{\beta\omega} - 1)}2\pi\delta(0) \tag{B.8}$$

$$\int W(t,t')e^{i\omega t'}dt' = \frac{1}{2\omega(e^{\beta\omega} - 1)}2\pi\delta(0) \tag{B.9}$$

So our two eigenvalues are

$$\lambda_+ = \frac{e^{\beta\omega}}{(e^{\beta\omega} - 1)} \tag{B.10}$$

$$\lambda_- = \frac{-1}{(e^{\beta\omega} - 1)} \tag{B.11}$$

Substituting these into

$$S = \sum_n \lambda_n \ln|\lambda_n| \tag{B.12}$$

we get

$$\begin{aligned} S &= \lambda_+ \ln|\lambda_+| + \lambda_- \ln|\lambda_-| \\ &= \frac{e^{\beta\omega}}{(e^{\beta\omega} - 1)} \ln(\frac{e^{\beta\omega}}{(e^{\beta\omega} - 1)}) - \frac{1}{(e^{\beta\omega} - 1)} \ln(\frac{1}{e^{\beta\omega} - 1}) \\ &= -\ln[1 - e^{-\beta\hbar\omega}] + \frac{e^{-\frac{\beta\omega}{2}}}{1 - e^{-\beta\hbar\omega}} \end{aligned} \tag{B.13}$$

We obtain the expected result.

Appendix C

Proof of S_A=S_B

If a Cauchy surface is divided into a subregion A and its complement B, then the reduced density matrix for region A is

$$\rho_A = Tr_B \rho \tag{C.1}$$

and the entanglement entropy corresponding to this reduced density matrix would be

$$S_A = -Tr \rho_A \ln \rho_A \tag{C.2}$$

When the system is in a pure state, $S_A = S_B$. This can be seen through the Schmidt decomposition theorem:

For any pure state ψ_{AB} there exist orthonormal sets $\{\psi_A\}$ and $\{\psi_B\}$ such that:

$$\psi_{AB} = \sum_n \lambda_n^{1/2} \psi_A^{(n)} \psi_B^{(n)} \tag{C.3}$$

where $\lambda_n^{1/2} > 0$ and $\sum_n \lambda_n = 1$. This holds even if $\mathcal{H}_A$ and $\mathcal{H}_B$ have different dimensionalities, and the range of the sum (C.3) is determined by the smaller Hilbert space. Now

$$\rho_A = Tr_B \psi_{AB} \psi_{AB}^\dagger = \sum_n \lambda_n \psi_A^{(n)} \psi_A^{(n)\dagger} \tag{C.4}$$

and

$$\rho_B = Tr_A \psi_{AB} \psi_{AB}^\dagger = \sum_n \lambda_n \psi_B^{(n)} \psi_B^{(n)\dagger} \tag{C.5}$$

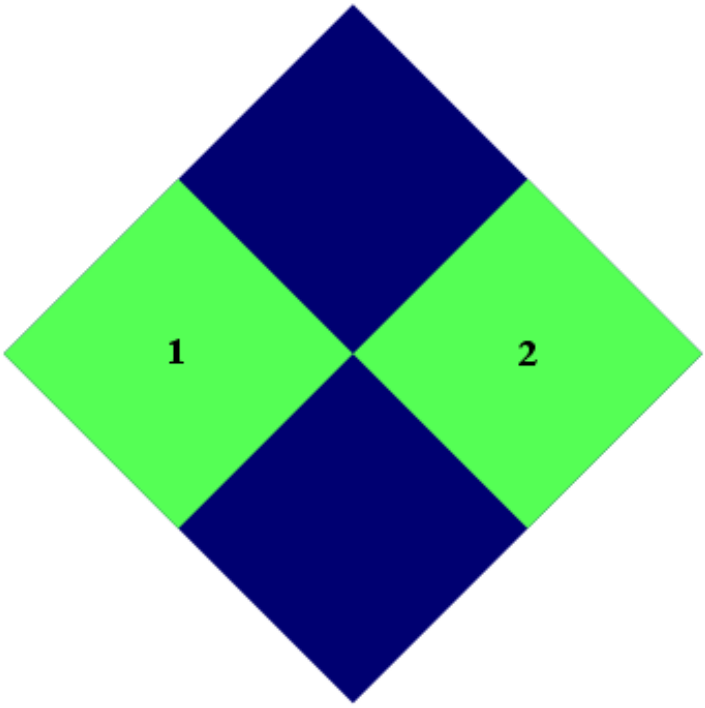

Figure C.1: A spacetime divided into two globally hyperbolic subregions 1 and 2.

Therefore since ρ_A and ρ_B have the same set of nonzero eigenvalues λ_n, we have that $S_A = S_B$.

We now derive a proof of this property of entanglement entropy, using the formula of Chapter 4. Let us divide the spacetime into two globally hyperbolic regions 1 and 2, as shown in figure C.1. We can write Δ in block diagonal form:

$$\Delta = \begin{pmatrix} \Delta_{11} & 0 \\ 0 & \Delta_{22} \end{pmatrix}$$

and W will have the general form:

$$W = \begin{pmatrix} W_{11} & W_{12} \\ W_{21} & W_{22} \end{pmatrix}$$

Let us define $M \equiv \Delta^{-1}W$. We know that M has eigenvalues 0 and 1, so $M = M^2$. From this we have that:

$$(\Delta_{11}^{-1}W_{11})^2 - \Delta_{11}^{-1}W_{11} = \Delta_{11}^{-1}W_{12}\Delta_{22}^{-1}W_{21} \tag{C.6}$$

$$(\Delta_{22}^{-1}W_{22})^2 - \Delta_{22}^{-1}W_{22} = \Delta_{22}^{-1}W_{21}\Delta_{11}^{-1}W_{12} \tag{C.7}$$

This pair of equations has the form of $Q_1^2 - Q_1 = RS$ and $Q_2^2 - Q_2 = SR$, where $Q_1 = \Delta_{11}^{-1}W_{11}$ and $Q_2 = \Delta_{22}^{-1}W_{22}$. Using the fact that the spectrum of RS equals that of SR, it must be that $Q_1^2 - Q_1$ and $Q_2^2 - Q_2$ have the same spectrum, which means:

$$\lambda_1^2 - \lambda_1 = \lambda_2^2 - \lambda_2 \qquad \rightarrow \qquad (\lambda_1 - \lambda_2)(\lambda_1 + \lambda_2 - 1) = 0 \tag{C.8}$$

$$\rightarrow \begin{cases} \lambda_1 = \lambda_2 \\ \lambda_1 = 1 - \lambda_2 = \lambda_2' \end{cases} \tag{C.9}$$

where the last line follows from the property that the eigenvalues of $\Delta_i^{-1}W_i$ come in pairs of λ and $1 - \lambda$. Finally, since $\Delta_{11}^{-1}W_{11}$ and $\Delta_{22}^{-1}W_{22}$ have the same spectrum, $S_1 = S_2$.

References

[1] E. Abdalla, M.C.B. Abdalla, and K.D. Rothe. *Non-perturbative methods in 2 dimensional quantum field theory*. World Scientific Pub Co Inc, 1991.

[2] Niayesh Afshordi, Michel Buck, Fay Dowker, David Rideout, Rafael D. Sorkin, and Yasaman K. Yazdi. A Ground State for the Causal Diamond in 2 Dimensions. *Journal of High Energy Physics*, 2012(10), 2012.

[3] N.D. Birrell and P.C.W. Davies. *Quantum fields in Curved Space*. Cambridge University Press, 1984.

[4] N.N. Bogoliubov, DV Shirkov, and E.M. Henley. Introduction to the theory of quantized fields. *Physics Today*, 13:40, 1960.

[5] Luca Bombelli, Joe Henson, and Rafael D. Sorkin. Discreteness without symmetry breaking: A theorem. *Mod. Phys. Lett.*, A24:2579–2587, 2009.

[6] Luca Bombelli, Rabinder K. Koul, Joohan Lee, and Rafael D. Sorkin. A quantum source of entropy for black holes. *Phys.Rev*, D34, 1986.

[7] Luca Bombelli, Joohan Lee, David Meyer, and Rafael Sorkin. Space-Time as a Causal Set. *Phys.Rev.Lett.*, 59:521–524, 1987.

[8] David G. Boulware. Quantum Field Theory in Schwarzschild and Rindler Spaces. *Phys.Rev.*, D11:1404, 1975.

[9] Pasquale Calabrese and John Cardy. Entanglement Entropy and Quantum Field Theory. *J. Stat. Mech*, (P06002), 2004.

[10] Pasquale Calabrese and John Cardy. Entanglement Entropy and Conformal Field Theory. *Journal of Physics A: Mathematical and Theoretical*, 42(50), 2009.

[11] Sidney R. Coleman. There are no Goldstone bosons in two dimensions. *Commun.Math.Phys.*, 31:259–264, 1973.

[12] P.C.W. Davies. Scalar particle production in Schwarzschild and Rindler metrics. *J.Phys.A*, A8:609–616, 1975.

[13] P.C.W. Davies and S.A. Fulling. Radiation from a moving mirror in two-dimensional space-time: conformal anomaly. *Proc.Roy.Soc.Lond.*, A348:393–414, 1976.

[14] Yves Decanini and Antoine Folacci. Hadamard Renormalization of the Stress-Energy Tensor for a Quantized Scalar Field in a General Spacetime of Arbitrary Dimension. *Physical Review D*, 78, 2008.

[15] P.A.M. Dirac. The Lagrangian in Quantum Mechanics. *Physikalische Zeitschrift der Sowjetunion*, 3:64–72, 1933.

[16] F. Dowker. Causal Sets and Discrete Spacetime. *AIP Conf.Proc.*, 861:79–88, 2006.

[17] Alessandro Fabbri and José Navarro-Salas. Modeling black hole evaporation. 2005.

[18] Manfried Faber and A.N. Ivanov. On the ground state of a free massless (pseudo)scalar field in two dimensions. 2002.

[19] Christopher J. Fewster and Rainer Verch. On a Recent Construction of "Vacuum-like" Quantum Field States in Curved Spacetime. 2012.

[20] S.A. Fulling. Aspects of Quantum Field Theory in Curved Spacetime. *London Math. Soc. Student Texts*, 17:1–315, 1989.

[21] Stephen A. Fulling. Nonuniqueness of canonical field quantization in Riemannian space-time. *Phys.Rev.*, D7:2850–2862, 1973.

[22] J.B. Hartle and S.W. Hawking. Path-integral derivation of black-hole radiance. *Physical Review D*, 13(8):2188, 1976.

[23] Song He and David Rideout. A Causal Set Black Hole. *Class.Quant.Grav.*, 26, 2009.

[24] Joe Henson. The Causal set approach to quantum gravity. In D. Oriti, editor, *Approaches to Quantum Gravity: Towards a New Understanding of Space and Time*. Cambridge University Press, 2006.

[25] Steven Johnston. Particle Propagators on Discrete Spacetime. *Class.Quant.Grav.*, 25:202001, 2008.

[26] Steven Johnston. Feynman Propagator for a Free Scalar Field on a Causal Set. *Phys.Rev.Lett.*, 103:180401, 2009.

[27] Steven Paul Johnston. *Quantum Fields on Causal Sets*. PhD thesis, Imperial College, 2010.

[28] T.F. Jordan. Linear operators for quantum mechanics. *American Journal of Physics*, 37:1166–1166, 1969.

[29] B.S. Kay and Robert M. Wald. Theorems on the Uniqueness and Thermal Properties of Stationary, Nonsingular, Quasifree States on Space-Times with a Bifurcate Horizon. *Phys. Rep 207*, pages 49–136, 1991.

[30] N. Afshordi, S. Aslanbeigi, and R. D. Sorkin. A Distinguished Vacuum State for a Quantum Field in a Curved Spacetime: Formalism, Features, and Cosmology. 2012.

[31] N. Afshordi, S. Aslanbeigi, M. Buck, F. Dowker and R.Sorkin. In preparation.

[32] Igor Novikov and Valeri Frolov. Black hole physics: basic concepts and new developments. *Springer*, 1998.

[33] W. Rindler. Kruskal Space and the Uniformly Accelerated Frame. *Am.J.Phys.*, 34:1174, 1966.

[34] W. Rindler. *Relativity: special, general, and cosmological*. Oxford University Press, USA, 2006.

[35] Shinsei Ryu and Tadashi Takayanagi. Holographic Derivation of Entanglement Entropy from AdS/CFT. *Phys. Rev. Lett.*, (96), 2006.

[36] Aram A. Saharian. Polarization of the Fulling-Rindler vacuum by uniformly accelerated mirror. *Class.Quant.Grav.*, 19, 2002.

[37] Mehdi Saravani, Rafael D. Sorkin, and Yasaman K. Yazdi. In Preparation.

[38] D.W. Sciama, P. Candelas, and D. Deutsch. Quantum Field Theory, Horizons and Thermodynamics. *Adv.Phys.*, 30:327–366, 1981.

[39] Rafael D. Sorkin. Forks in the road, on the way to quantum gravity. *Int.J.Theor.Phys.*, 36:2759–2781, 1997.

[40] Rafael D. Sorkin. Causal sets: Discrete gravity (notes for the valdivia summer school). In Andrés Gomberoff and Don Marolf, editors, *Lectures on Quantum Gravity, Proceedings of the Valdivia Summer School, Valdivia, Chile, January 2002*. Plenum, 2005.

[41] Rafael D. Sorkin. Does locality fail at intermediate length-scales? In D. Oriti, editor, *Approaches to Quantum Gravity: Towards a New Understanding of Space and Time*. Cambridge University Press, 2006.

[42] Rafael D. Sorkin. Scalar Field Theory on a Causal Set in Histories Form. *J.Phys.Conf.Ser.*, 306:012017, 2011.

[43] Rafael D. Sorkin. Expressing Entropy Globally in Terms of (4D) Field-Correlations. arXiv:1205.2953, 2012.

[44] MR Speigel. The summation of series involving roots of transcendental equations and related applications. *Journal of Applied Physics*, 24(9):1103–1106, 1953.

[45] M.H. Stone. *Linear transformations in Hilbert space and their applications to analysis*, volume 15. American Mathematical Society, 1979.

[46] W.G. Unruh. Notes on Black Hole Evaporation. *Phys.Rev.*, D14:870, 1976.

[47] Robert M. Wald. On Particle Creation by Black Holes. *Commun.Math.Phys.*, 45:9–34, 1975.

[48] Robert M. Wald. General Relativity. 1984. The University of Chicago Press, 1984.

[49] Robert M. Wald. Quantum Field Theory in Curved Space-time and Black Hole Thermodynamics. 1995. University of Chicago Press.

[50] Robert M. Wald. The Formulation of Quantum Field Theory in Curved Spacetime. 2009. arXiv0907.0416.